

1 ***Plasmodium* PIMMS43 is required for ookinete evasion of the**  
2 **mosquito complement-like response and sporogonic**  
3 **development in the oocyst**

4  
5  
6 Chiamaka V. Ukegbu<sup>1¶</sup>, Maria Giorgalli<sup>1¶</sup>, Sofia Tapanelli<sup>1</sup>, Luisa D.P. Rona<sup>1#a</sup>, Amie  
7 Jaye<sup>1</sup>, Claudia Wyer<sup>1</sup>, Fiona Angrisano<sup>1</sup>, Andrew M. Blagborough<sup>1#b</sup>, George K.  
8 Christophides<sup>1\*&</sup>, Dina Vlachou<sup>1\*&</sup>

9  
10  
11 <sup>1</sup> Department of Life Sciences, Imperial College London, London, UK

12  
13 <sup>#a</sup> Current address: Department of Cell Biology, Embryology and Genetics, Federal University of  
14 Santa Catarina, Florianopolis, Brazil & National Council for Scientific and Technological  
15 Development, National Institute of Science and Technology in Molecular Entomology, Rio de  
16 Janeiro, Brazil

17  
18 <sup>#b</sup> Current address: Division of Microbiology and Parasitology, Department of Pathology,  
19 University of Cambridge, Cambridge, UK

20  
21 \*Corresponding authors:

22 Emails: [g.christophides@imperial.ac.uk](mailto:g.christophides@imperial.ac.uk) (GKC) and [d.vlachou@imperial.ac.uk](mailto:d.vlachou@imperial.ac.uk) (DV)

23  
24 <sup>¶</sup> These authors contributed equally to this work

25 <sup>&</sup> These authors also contributed equally to this work and are joint senior authors

26  
27 **Short title:** Malaria parasite evasion of mosquito immune response

28

## 29 **Abstract**

30 Malaria transmission requires *Plasmodium* parasites to successfully infect a female *Anopheles*  
31 mosquito, surviving a series of robust innate immune responses. Understanding how parasites evade  
32 these responses can highlight new ways to block malaria transmission. We show that ookinete and  
33 sporozoite surface protein PIMMS43 is required for *Plasmodium* ookinete evasion of the *Anopheles*  
34 *coluzzii* complement-like system and for sporogonic development in the oocyst. Disruption of *P.*  
35 *berghei* PIMMS43 triggers robust complement activation and ookinete elimination upon mosquito  
36 midgut traversal. Silencing the complement-like system restores ookinete-to-oocyst transition.  
37 Antibodies that bind PIMMS43 interfere with parasite immune evasion when ingested with the  
38 infectious blood meal and significantly reduce the prevalence and intensity of infection. PIMMS43  
39 genetic structure across African *P. falciparum* populations indicates allelic adaptation to sympatric  
40 vector populations. These data significantly add to our understanding of mosquito-parasite  
41 interactions and identify PIMMS43 as a target of interventions aiming at malaria transmission  
42 blocking.

43

## 44 **Author summary**

45 Malaria is a devastating disease transmitted among humans through mosquito bites. Mosquito  
46 control has significantly reduced clinical malaria cases and deaths in the last decades. However, as  
47 mosquito resistance to insecticides is becoming widespread impacting on current control tools, such  
48 as insecticide impregnated bed nets and indoor spraying, new interventions are urgently needed,  
49 especially those that target disease transmission. Here, we characterize a protein found on the  
50 surface of malaria parasites, which serves to evade the mosquito immune system ensuring disease  
51 transmission. Neutralization of PIMMS43, either by eliminating it from the parasite genome or by  
52 pre-incubating parasites with antibodies that bind to the protein, is shown to inhibit mosquito  
53 infection by malaria parasites. Differences in PIMMS43 detected between malaria parasite  
54 populations sampled across Africa suggest that these populations have adapted for transmission by  
55 different mosquito vectors that are also differentially distributed across the continent. We conclude  
56 that interventions targeting PIMMS43 could block malaria parasites inside mosquitoes before they  
57 can infect humans.

58

## 59 **Keywords**

60 Malaria transmission | mosquito innate immunity | complement-like response | midgut epithelium  
61 traversal | parasite immune evasion | transmission blocking vaccines | mosquito population  
62 replacement

63

## 64 **Introduction**

65 Enhanced vector control significantly reduced malaria cases in recent years and together with  
66 effective medicines and better health care decreased the number of malaria-associated deaths.  
67 However, these measures have reached their maximum capacity, as resistance to insecticides used  
68 in bed-net impregnation and indoors residual spraying is now widespread and mosquito biting and  
69 resting behaviors have changed in response to these measures. Therefore, additional tools for  
70 malaria control are needed, especially ones that target disease transmission.

71 Mosquito acquisition of *Plasmodium* parasites commences when a female *Anopheles* mosquito  
72 ingests gametocyte-containing blood from an infected person. In the mosquito midgut lumen,  
73 gametocytes mature and produce gametes. Fertilization of gametes leads to zygotes that soon  
74 develop to ookinetes and traverse the midgut epithelium. At the midgut basal sub-epithelial space,  
75 ookinetes differentiate into replicative oocysts wherein hundreds of sporozoites develop within a  
76 period of 1-2 weeks. Upon release into the haemocoel, sporozoites migrate to the salivary glands to  
77 infect a new host upon a next mosquito bite.

78 Inside the mosquito, parasites are attacked by an array of immune responses [1, 2]. Most parasite  
79 losses occur during the ookinete-to-oocyst transition [3, 4]. Ookinete traversal of the mosquito  
80 midgut leads to activation of JNK (c-Jun N-terminal kinase) signaling, inducing apoptosis of the  
81 invaded cells. This response involves various effectors including heme peroxidase 2 (HPX2) and  
82 NADPH oxidase 5 (NOX5) that potentiate nitration of ookinetes that are henceforth marked for  
83 elimination by reactions of the mosquito complement-like system [5, 6]. These reactions are  
84 triggered upon ookinete exit at the midgut sub-epithelial space encountering the hemolymph that  
85 carries the complement-like system.

86 The hallmark of the mosquito complement-like system is the C3-like factor, TEP1 [7, 8]. A  
87 proteolytically processed form of TEP1, TEP1<sub>cut</sub>, circulates in the hemolymph as a complex with  
88 LRIM1 and APL1C [9, 10]. Upon parasite recognition, TEP1<sub>cut</sub> is released from the complex and  
89 attacks the ookinete triggering *in situ* assembly of a TEP1 convertase that locally processes TEP1  
90 molecules that bind to the ookinete causing lysis and, in some cases, melanization [11]. These  
91 reactions are regulated by CLIP-domain serine proteases and their inactive homologs [11, 12].  
92 Ookinete clearance is assisted by actin-mediated cellular responses of invaded epithelial cells [13].

93 The characterization of *Plasmodium falciparum* Pfs47 as a key player in parasite evasion of the  
94 mosquito complement-like response has opened new avenues to dissect the mechanisms parasites  
95 employ to endure or indeed evade the mosquito immune response. GPI-anchored Pfs47 is shown to  
96 interfere with activation of JNK signaling, aiding ookinetes to escape nitration and subsequent  
97 complement-mediated attack [14, 15]. This function is shared by the Pfs47 ortholog in the rodent  
98 malaria parasite *Plasmodium berghei* [16], which was earlier thought to be solely involved in  
99 fertilization [17].

100 Our transcriptomic profiling of field *P. falciparum* isolates from Burkina Faso in the midgut of  
101 sympatric *A. coluzzii* (previously *Anopheles gambiae* M form) and *Anopheles arabiensis*  
102 mosquitoes (unpublished) and a laboratory *P. berghei* strain in the midgut of *A. coluzzii* [18]  
103 identified hundreds of genes exhibiting conserved and differential expression during gametocyte to  
104 oocyst development. Several of them encoding putatively secreted or membrane-associated proteins  
105 were made part of a screen to identify genes that function during parasite infection of the mosquito  
106 midgut. These genes were given a candidate gene number preceded by the acronym PIMMS for  
107 *Plasmodium* Infection of the Mosquito Midgut Screen. We previously characterized PIMMS2 that  
108 encodes a subtilisin-like protein involved in midgut traversal [19]. Here, we report the  
109 characterization of *P. falciparum* and *P. berghei* PIMMS43 that encodes a membrane-bound protein  
110 found on the surface of ookinetes and sporozoites. The gene was firstly reported in *P. berghei* to be  
111 a target of the transcription factor AP2-O and have a role in mosquito midgut invasion and oocyst  
112 development, and was named POS8 [20]. A later study by another group reported the gene as being  
113 important for ookinete maturation, designating it as PSOP25 [21]. Here we demonstrate that  
114 PIMMS43 has no detectable function in ookinete maturation or mosquito midgut invasion but plays  
115 a key role in ookinete evasion of the mosquito complement-like response. We show that disruption  
116 of PIMMS43 leads to robust complement activation and ookinete elimination upon completion of  
117 midgut traversal and before their transformation to oocysts. When the complement system is  
118 inactivated, oocyst transformation is restored but sporogony cannot be completed, as the gene is  
119 also essential for sporozoite development. Parallel analysis of thousands of African *P. falciparum*

120 parasites reveals clear genetic differentiation between populations sampled from West or Central  
121 and East African countries, inferring parasite adaptation to sympatric vector populations. We further  
122 demonstrate that *A. coluzzii* ingestion of antibodies against *P. falciparum* PIMMS43 leads to strong  
123 inhibition of oocyst development. The discoveries of PIMMS43 here and P47 previously open new,  
124 unprecedented avenues for understanding parasite immune evasion in the vector and development  
125 of novel interventions for malaria transmission blocking.

126

## 127 **Results and discussion**

### 128 **Identification of *PIMMS43***

129 *P. falciparum* (PF3D7\_0620000) and *P. berghei* (PBANKA\_1119200) *PIMMS43* encode deduced  
130 proteins of 505 and 350 amino acids, respectively. N-terminal signal peptides (amino acids 1-25 for  
131 PfPIMMS43 and 1-22 for PbPIMMS43) and C-terminal transmembrane domains (amino acids 482-  
132 504 for PfPIMMS43 and 327-350 for PbPIMMS43) are predicted for both proteins. The  
133 transmembrane domains are predicted by PredGPI to also contain signals for attachment of a  
134 glycosyl-phosphatidylinositol (GPI) lipid anchor with 99% probability.

135 PIMMS43 is conserved among species of the *Plasmodium* genus. All orthologs are predicted to  
136 contain the N-terminal signal peptide and C-terminal transmembrane domain, as well as a  
137 conserved pair of cysteine residues adjacent to the C-terminus (**Figure S1**). PbPIMMS43 exhibits a  
138 68% sequence identity with orthologs in other rodent parasites, i.e. *P. yoelii* and *P. chabaudi*, and  
139 27% and 24% with *P. falciparum* and *P. vivax* PIMMS43, respectively. PfPIMMS43 and  
140 PvPIMMS43 contain a 60-180 non-conserved amino acid insertion with no obvious sequence  
141 similarity between them, which are therefore likely to have occurred independently. Another  
142 shorter, non-conserved insertion towards the C-terminus of *P. vivax* and *P. knowlesi* PIMMS43  
143 includes tandem repeats of Glycine-Serine-Glutamine-Alanine-Serine (GSQAS).

### 144 ***PIMMS43* transcription profiles and protein expression**

145 DNA microarray profiling of *A. coluzzii* and *A. arabiensis* midguts infected with *P. falciparum* field  
146 isolates in Burkina Faso revealed that *PfPIMMS43* (referred to in figures as *Pfc43*) shows  
147 progressively increased transcription that peaks 24 hours post mosquito blood feeding (hpbf;  
148 **Figure 1A, left panel**). These data were corroborated by laboratory *P. falciparum* NF54 infections  
149 of *A. coluzzii* using RT-PCR (**Figure 1A, right panel**). Low levels of *PfPIMMS43* transcripts were  
150 also detected in in vitro cultured gametocytes but not in in vitro cultured asexual blood stage (ABS)  
151 parasites, indicating that *PfPIMMS43* transcription begins in gametocytes and peaks in zygotes and  
152 ookinetes. Transcripts were not detected in oocysts 10 days post mosquito blood feeding but  
153 reappeared in mosquito salivary glands, indicative of *PfPIMMS43* re-expression in sporozoites.

154 We examined whether the *P. berghei* *PIMMS43* ortholog (referred to in figures as *Pbc43*) shows  
155 expression profile similar to *PfPIMMS43*, using quantitative real-time RT-PCR (qRT-PCR; **Figure**  
156 **1B, left panel**) and RT-PCR (**Figure 1B, right panel**). In these assays, we used the *P. berghei* line  
157 *ANKA507m6c11* that constitutively expresses GFP [22], hereafter referred to as *c507*, as well as the  
158 non-gametocyte producing ANKA 2.33 (NGP) as a control in the RT-PCR assay. The results  
159 revealed low levels of *PbPIMMS43* transcripts in mixed blood stages (MBS) and purified *c507*  
160 gametocytes, which together with absence of transcripts from NGP MBS indicated that  
161 *PbPIMMS43* transcription begins in gametocytes, similar to *PfPIMMS43*. Also similar to  
162 *PfPIMMS43*, *PbPIMMS43* transcript levels were very high 24 hpbf as well as in purified in vitro  
163 produced ookinetes, indicating high *PbPIMMS43* transcription in ookinetes. Lower transcript levels

164 were detected 2 days post blood feeding (dpbf), presumably due to ookinetes retained in the blood  
165 bolus and the midgut epithelium and/or low-level expression in young oocysts. No *PbPIMMS43*  
166 transcripts were detected in mature oocysts 10 dpbf, but strong *PbPIMMS43* re-expression was  
167 observed in salivary gland sporozoites. These data together indicate that *P. falciparum* and *P.*  
168 *berghei* *PIMMS43* exhibit similar transcription patterns starting in gametocytes, peaking in  
169 ookinetes, pausing in oocysts and restarting in salivary gland sporozoites.

170 To investigate *PbPIMMS43* protein expression, we raised rabbit polyclonal antibodies against a  
171 codon-optimized fragment of the protein (amino acids 22-327) expressed in *E. coli* cells ( $\alpha$ -  
172 *Pbc43*<sup>opt</sup>), and a native protein fragment (amino acids 22-331) expressed in insect *Spodoptera*  
173 *frugiperda* Sf9 cells ( $\alpha$ -*Pbc43*<sup>Sf9</sup>). Both recombinant proteins lacked the predicted signal peptide  
174 and C-terminal transmembrane domain. We also generated a genetically modified *c507 P. berghei*  
175 line, designated  $\Delta c43$ , where 50% of the *PbPIMMS43* coding region was replaced with a modified  
176 *Toxoplasma gondii* pyrimethamine resistance expression cassette (*TgDHFR*; **Figure S2A**).  
177 Integration of the disruption cassette was confirmed by PCR and pulse field gel electrophoresis  
178 (**Figure S2B-C**). RT-PCR assays confirmed that *PbPIMMS43* transcripts could no longer be  
179 detected in gametocytes, ookinetes and sporozoites of the  $\Delta c43$  line that was henceforth used as a  
180 negative control in protein expression experiments (**Figure 1B, right panel**). Western blot analysis  
181 was performed in total, triton-soluble protein extracts prepared under reducing conditions from  
182 MBS, purified gametocytes and in vitro cultured ookinetes of the *c507* and  $\Delta c43$  *P. berghei* lines  
183 (**Figure 1C**). Two clear bands of approximately 37 and 75 kDa were detected in ookinete extracts  
184 of the *c507* line. The former band matches the predicted molecular weight of *PbPIMMS43*  
185 monomer and the latter band could correspond to *PbPIMMS43* dimer, either a homodimer formed  
186 upon disulfide bonding of the conserved pair of cysteine residues or a heterodimer. Indeed, under  
187 strong reducing conditions, the 75 kDa was resolved in a single 37 kDa band whereas under non-  
188 reducing conditions only the 75 kDa could be detected (**Figure 1D**). This assay was combined with  
189 membrane-fractionation of total in vitro ookinete extracts, which revealed that both bands were only  
190 observed in the insoluble fraction and the fraction solubilized by triton, but not in the soluble (triton  
191 non-treated) fraction. These data indicate membrane association of *PbPIMMS43*, in accordance  
192 with the prediction of a transmembrane domain and a GPI anchor.

193 We also raised a rabbit polyclonal antibody against a codon-optimized coding fragment of *P.*  
194 *falciparum* *PIMMS43* (amino acids 25-481) expressed in *E. coli* cells and lacking the predicted  
195 signal peptide and C-terminal transmembrane domain ( $\alpha$ -*Pfc43*<sup>opt</sup>). We examined the affinity and  
196 specificity of this antibody by generating and using a *P. berghei c507* transgenic line (*Pb*<sup>*Pfc43*</sup>)  
197 where *PbPIMMS43* was replaced by *PfPIMMS43* (**Figure S3A**). PCR genotypic analysis confirmed  
198 successful modification of the endogenous *PbPIMMS43* genomic locus (**Figure S3B**), and RT-PCR  
199 analysis confirmed that *PfPIMMS43* is transcribed in in vitro cultured *P. berghei* ookinetes (**Figure**  
200 **S3C**). Western blot analysis of total protein extracts prepared from purified in vitro cultured *Pb*<sup>*Pfc43*</sup>  
201 ookinetes using the  $\alpha$ -*Pfc43*<sup>opt</sup> antibody revealed a strong band of approximately 60 kDa,  
202 corresponding to the predicted molecular weight of the deduced *PfPIMMS43* protein (**Figure S3D**).  
203 This band was absent from *c507* and  $\Delta c43$  protein extracts confirming the specificity of the  $\alpha$ -  
204 *Pfc43*<sup>opt</sup> antibody. It is noteworthy that, in contrast to what was observed with the *PbPIMMS43*  
205 protein, the results did not show dimerization of the ectopically expressed *PfPIMMS43* protein  
206 when the analysis was done under non-reducing conditions (**Figure S3D**).

## 207 **PIMMS43 protein sub-cellular localization**

208 We used the  $\alpha$ -*Pfc43*<sup>opt</sup> antibody in indirect immunofluorescence assays to investigate the sub-  
209 cellular localization of *PfPIMMS43* in *P. falciparum* NF54 parasite stages. Antibodies against the  
210 female gametocyte and ookinete surface protein *Pfs25* and the sporozoite surface protein *PfCSP*  
211 (Circumsporozoite protein) were used as stage-specific controls. The results showed that



212 PfPIMMS43 prominently localizes on the surface of female gametocytes or early stage zygotes  
213 found in the *A. coluzzii* blood bolus 1 hpbfb, as well as on the surface of ookinetes traversing the  
214 mosquito midgut epithelia and sporozoites found in the mosquito salivary gland lumen at 25 hpbfb  
215 and 16 dpbf, respectively (**Figure 2A**). No staining with the  $\alpha$ -Pfc43<sup>opt</sup> antibody was observed in in  
216 vitro cultured ABS or gametocytes (data not shown) suggesting that expression of PfPIMMS43  
217 protein starts after fertilization. No signal was detected with the  $\alpha$ -Pfc43<sup>opt</sup> rabbit pre-immune serum  
218 that was used as a negative control.

219 Immunofluorescence assays of *P. berghei* c507 and control  $\Delta$ c43 parasite stages using the  $\alpha$ -  
220 Pbc43<sup>opt</sup> antibody revealed that, similarly to its *P. falciparum* ortholog, PbPIMMS43 localizes on  
221 the surface of *A. coluzzii* midgut-traversing ookinetes and salivary gland sporozoites (**Figure 2B**).  
222 For the control  $\Delta$ c43 line, which as reported below does not develop beyond the ookinete stage,  
223 sporozoites were obtained from infections of *LRIM1* knockdown (kd) mosquitoes (see below). Like  
224 PfPIMMS43, and despite the presence of transcripts, no signal was detected in gametocytes. Also,  
225 no PbPIMMS43 signal was detected in early stage zygotes present in the blood bolus 1 hpbfb,  
226 suggesting that translation starts later during ookinete development. In both species, the protein was  
227 detectable on the surface of 2-day old oocysts found on the *A. coluzzii* midgut cell wall and  
228 reappeared in sporozoites found in mature *P. falciparum* oocysts 11 dpbf and *P. berghei* oocysts 15  
229 dpbf (**Figure S4**).

### 230 **Phenotypic characterization of *P. berghei* lacking *PIMMS43***

231 We phenotypically characterized the *P. berghei*  $\Delta$ c43 line generated as described above. Consistent  
232 with the *PbPIMMS43* expression data,  $\Delta$ c43 parasites exhibited normal development in mouse  
233 blood stages (data not shown). Both, male gametocyte activation, as measured by counting  
234 exflagellation centers (**Figure 3A**), and macrogametocyte-to-ookinete conversion rate, both in vitro  
235 and in the *A. coluzzii* midgut lumen (**Figure 3B**), were comparable to the c507 parental line,  
236 indicating that no developmental defects are accompanying the parasite gametocyte-to-ookinete  
237 developmental transition. However, no oocysts were detected in *A. coluzzii* midguts at 3, 5, 7 or 10  
238 dpbf, indicating complete abolishment of oocyst formation (**Figure 3C**, **Table S1**). Thus, oocyst  
239 and salivary gland sporozoites were never observed, and transmission to mice following mosquito  
240 bite-back was abolished (**Table S2**).

241 To validate the specificity of this phenotype, we reintroduced *PbPIMMS43* into the  $\Delta$ c43 locus by  
242 replacing the *TgDHFR* gene cassette with the *PbPIMMS43* coding sequence flanked by its 5' and 3'  
243 untranslated regions (UTRs) and followed by the human *DHFR* gene cassette (**Figure S5A**).  
244 Successful integration was confirmed with PCR (**Figure S5B**). Phenotypic characterization of the  
245 resulting  $\Delta$ c43::c43<sup>wt</sup> parasite line in *A. coluzzii* infections showed that oocyst development was  
246 fully restored (**Figure S5C**, **Table S1**).

247 These data were in disagreement with those reported previously, which showed that *PSOP25*  
248 knockout (ko) parasites exhibit reduced ookinete conversion rates and defective ookinete  
249 maturation [21]. To investigate this discrepancy, we generated a new *PIMMS43* ko ( $\Delta$ c43<sup>red</sup>) line in  
250 the 1804c11 (c1804) *P. berghei* line that constitutively expresses mCHERRY [23], using the same  
251 disruption vector (PbGEM-042760) as the one used by the authors of the previous study, which  
252 leads to 74% removal of the gene coding region (**Figure S6A-B**). Phenotypic analysis showed that  
253  $\Delta$ c43<sup>red</sup> parasites show normal ookinete conversion rates both in vitro and in *A. coluzzii* infections  
254 but produced no oocysts (**Figure S6C**), a phenotype identical to that of the  $\Delta$ c43 line. Similar  
255 results were obtained in infections of *A. stephensi*, the vector of choice in the previous studies  
256 (**Figure S6D**). Interestingly, the number of oocysts in *A. stephensi* infections was very small but not  
257 zero. This is consistent with the findings by Kaneko and co-workers [20], as well as with the  
258 general understanding that the *A. stephensi* Nijmegen strain, which was genetically selected for high

259 susceptibility to parasite infections [24], has a less robust immune response than *A. coluzzii*.  
260 Nonetheless, no sporozoites were detected in the *A. stephensi* midgut 15 dpbf (**Figure S6E**).

### 261 ***Δc43* ookinete killing by the mosquito complement-like response**

262 We examined whether the *PIMMS43* ko phenotype was due to defective ookinete motility and,  
263 hence, capacity to invade or traverse the mosquito midgut epithelium. Ookinete motility assays  
264 showed that *Δc43* ookinetes moved on Matrigel with average speed that was not significantly  
265 different from *c507* ookinetes (**Figure 3D**).

266 Next, a potential defect in midgut epithelium invasion and traversal was assessed in infections of *A.*  
267 *coluzzii* where *CTL4* (*C-type lectin 4*) was silenced by RNA interference. *CTL4* kd leads to  
268 melanization of ookinetes at the midgut sub-epithelial space upon epithelium traversal providing a  
269 powerful means to visualize and enumerate ookinetes that successfully traverse the midgut  
270 epithelium. The number of *Δc43* melanized ookinetes was comparable to that of the *c507* line that  
271 was used as control (**Figure 3E, Table S3**), indicating that *Δc43* ookinetes successfully traverse the  
272 midgut epithelium but fail to transform to oocysts.

273 A similar phenotype was previously reported for P47 ko parasites that are eliminated by mosquito  
274 complement-like responses upon emergence at the midgut sub-epithelial space [16]. To examine  
275 whether the same applies to *Δc43* parasites, we infected *A. coluzzii* mosquitoes in which genes  
276 encoding two major components of the complement-like system, *TEP1* and *LRIMI*, were  
277 individually silenced. Enumeration of oocysts 10 dpbf, and comparison with control mosquitoes  
278 injected with *LacZ* double stranded RNA, revealed that *Δc43* oocyst development was partly  
279 restored in both *TEP1* and *LRIMI* kd mosquitoes (**Figure 4A, Table S4**).

280 We investigated whether ookinete attack by the complement-like response is responsible for the  
281 observed *Δc43* phenotype by staining midgut tissues of *A. coluzzii* mosquitoes infected with control  
282 *c507* or *Δc43* parasites with antibodies against P28 and TEP1 at 28-30 hpbpf. Whilst P28 is found on  
283 the surface of all ookinetes, both live and dead, TEP1 only binds ookinetes targeted for elimination  
284 [7]. The results showed that 86% of *Δc43* ookinetes showed TEP1 staining, which was significantly  
285 higher than the 79% of *c507* ookinetes showing TEP1 staining ( $P < 0.005$ ; **Figure 4B, Table S5**).

286 Together these data indicate that absence of *PIMMS43* does not affect the capacity of ookinetes to  
287 invade and traverse the mosquito midgut epithelium; instead, it is required for evasion of the  
288 mosquito complement-like response. The observations that *Δc43* oocyst numbers are still inferior to  
289 *wt* parasite oocyst numbers in *TEP1* and *LRIMI* kd mosquitoes and that TEP1 binding is not solely  
290 responsible for the almost full attrition of ookinete-to-oocyst transformation suggest that immune  
291 responses additional to the complement-like response mediate the killing of *Δc43* ookinetes. Indeed,  
292 it has been previously shown that some dead ookinetes in the midgut epithelium are not bound by  
293 TEP1, indicating alternative means employed by the mosquito to kill *Plasmodium* ookinetes [7].  
294 Other mosquito immune factors, such as fibrinogen-related proteins (FREPs or FBNs) and LRRD7,  
295 are also important for midgut infection [25, 26]. Of these, FBN9 is shown to co-localize with  
296 ookinetes in the midgut epithelium, probably mediating their death [26]. Any such mechanism  
297 employed by the mosquito to kill *Δc43* ookinetes would have to be TEP1-independent. Since TEP1  
298 binding is potentiated by prior marking of ookinetes by effector reactions of the JNK pathway [5,  
299 6], it is plausible that *Δpbc43* ookinetes are excessively marked for death either by the same  
300 mechanism observed for *Pfs47* null mutants or an independent mechanism. Nonetheless, all the  
301 above scenarios suggest that *PIMMS43*, like P47, directly interfere with the mosquito immune  
302 response promoting ookinete survival. Alternatively, *PIMMS43* may confer a fitness advantage to  
303 ookinetes, allowing them to endure the mosquito immune response, therefore mediating indirect  
304 evasion of the immune system.

## 305 **Oocyst development and sporozoite infectivity of *Δc43* parasites**

306 We observed that rescued *Δc43* oocysts in *LRIMI* or *TEPI* kd mosquitoes were morphologically  
307 variable and smaller in size compared to *c507* oocysts (**Figure 4C**). At 14 and 16 dpbf the average  
308 *Δc43* oocyst diameter was 20.1 and 17.2 μm compared to 27.4 and 30.9 μm of *c507* oocysts,  
309 respectively (**Figure 4D**). All pairwise comparisons were statistically significant and revealed that  
310 the mean *Δc43* oocyst diameter at 16 dpbf was smaller than 14 dpbf, indicating progressive  
311 degeneration of *Δc43* oocysts. Similar data were obtained with *TEPI* kd mosquitoes (data not  
312 shown). In addition, *Δc43* oocysts in *LRIMI* and *TEPI* kd mosquitoes yielded a very small number  
313 of midgut and salivary gland sporozoites compared to *c507* oocysts, and the ratio of salivary gland  
314 to midgut sporozoites was significantly smaller for *Δc43* compared to control *c507* parasites (**Table**  
315 **S6**). The few *Δc43* sporozoites that reached the salivary glands could not be transmitted to mice by  
316 mosquito bite.

317 These data suggested that *Δc43* parasites are defective not only with respect to ookinete toleration  
318 of the mosquito complement-like response but also with sporozoite development and infectivity.  
319 We investigated whether bypassing midgut invasion, a process in which ookinetes are marked for  
320 elimination by complement-like reactions, could rescue *Δc43* sporozoite development and  
321 transmission to a new host. In vitro produced *Δc43* and control *c507* ookinetes were injected into  
322 the haemocoel of *A. coluzzii* mosquitoes, and sporozoites found in the mosquito salivary glands 21  
323 days later were enumerated. The results revealed that no *Δc43* sporozoites could be detected in the  
324 mosquito salivary glands, and consequently, mosquitoes inoculated with *Δc43* ookinetes could not  
325 transmit malaria to mice, in contrast to mosquitoes inoculated with *c507* ookinetes (**Table S7**).  
326 These data confirmed that PbPIMMS43 has an additional, essential function in sporozoite  
327 development.

328 Next, we investigated whether PfPIMMS43 could complement the function of its *P. berghei*  
329 ortholog, by infecting naïve *A. coluzzii* mosquitoes with the *Pb<sup>Pfc43</sup>* parasite line and counting the  
330 number of oocysts detected in the mosquito midguts. Infections with *c507* and *Δc43* parasites  
331 served as positive and negative controls, respectively. The results showed that the *Pb<sup>Pfc43</sup>* line  
332 exhibited an intermediate phenotype compared to *c507* and *Δc43* both in terms of both infection  
333 prevalence and intensity (**Figure S3E, Table S4**). Oocysts were morphologically variable and  
334 smaller in size compared to *c507* oocysts and produced a very small number of midgut and salivary  
335 gland sporozoites (data not shown), resembling the phenotype obtained with *Δc43* infections  
336 following silencing of the mosquito complement-like system. We examined whether this partial  
337 complementation phenotype could be affected upon *LRIMI* silencing. Indeed, a significant increase  
338 in both the infection prevalence and oocyst numbers was observed (**Figure S3E, Table S4**), yet  
339 oocysts remained small and morphologically variable and produced few sporozoites (data not  
340 shown). These results suggest that PfPIMMS43 can only partly complement the function of its  
341 PbPIMMS43 ortholog and corroborate the dual function of PIMMS43 in ookinete to oocyst  
342 transition and in oocyst maturation and sporozoite development, respectively.

## 343 **RNA sequencing of *Δc43* parasites and mosquito responses**

344 We carried out RNA next generation sequencing of *P. berghei Δc43* and *c507* infected *A. coluzzii*  
345 midguts at 1 and 24 hpbpf to investigate the molecular basis of the *Δc43* phenotype during mosquito  
346 midgut infection. *P. berghei* and *A. coluzzii* transcriptomes were processed separately, and  
347 comparatively analyzed at each time point for each parasite line (**Figure 5; Dataset S1**). Three  
348 independent biological replicates and three technical replicates for each biological replicate were  
349 performed.

350 At 1 hpbpf, when asexual parasite stages and gametocytes are sampled from the mosquito blood  
351 bolus, almost all 17 changes registered between *Δc43* and *c507* parasites concerned genes belonging



352 to multigene families (*pir*, *fam-a* and *fam-b*) and 28S ribosomal RNA subunits, which are thought to  
353 exhibit differential expression between clonal parasite lines (**Figure 5A, left panel**). *PbPIMMS43*  
354 was downregulated in the  $\Delta c43$  line, consistent with its transcription in gametocytes. However, as  
355 many as 163 genes were differentially regulated between the  $\Delta c43$  and *c507* parasites at 24 hpbf, of  
356 which 137 were downregulated (41 at least 2-fold) and 26 were upregulated (9 at least 2-fold)  
357 (**Figure 5A, right panel**). Gene ontology (GO) analysis revealed several biological processes and  
358 three cellular component terms that were significantly enriched in the differentially regulated gene  
359 set (**Table S8**). All GO terms were related to host-parasite interactions, including micronemal  
360 secretion, entry into host cell and parasite movement. Genes included in this list encode known  
361 ookinete secreted or membrane associated proteins such as CTRP, SOAP, MAEBL, WARP, PLP3-  
362 5, PIMMS2, HADO, PSOP1, PSOP7, PSOP26, GAMA (aka PSOP9) and others, all of which were  
363 downregulated in  $\Delta c43$  parasites. The expression of the oocyst capsule protein *Cap380* gene that  
364 begins in ookinetes was also affected [27].

365 These data could be explained by a smaller ratio of ookinetes to other parasite stages sampled from  
366 the midgut at 24 hpbf in  $\Delta c43$  infections compared to *c507* infections. Although the data from the  
367 ookinete melanization assays showed that differences between  $\Delta c43$  and *c507* in ookinete numbers  
368 exiting the mosquito midgut were not statistically significant ( $P=0.0947$ ), these differences were  
369 almost 2-fold both with regards to median and arithmetic mean (**Table S3**). This difference could  
370 justify the observed 2-fold downregulation of genes showing enriched expression in ookinetes. A  
371 second hypothesis is that  $\Delta c43$  parasites exhibit deficient expression of genes involved in ookinete  
372 secretions and movement. The latter hypothesis is less appealing, as it is difficult to explain how  
373 absence of a membrane-associated protein without obvious signaling domains could affect the  
374 transcription of all other genes. However, the two hypotheses are not mutually exclusive, and both  
375 indicate that disruption of *PIMMS43* leads to compromised ookinete fitness.

376 Analysis of *A. coluzzii* midgut transcriptional responses to infection by  $\Delta c43$  compared to *c507*  
377 identified 192 and 122 differentially regulated genes at 1 and 24 hpbf, respectively (**Dataset S2**). At  
378 1 hpbf, 154 (88 over 2-fold) genes were downregulated and 38 (21 over 2-fold) were upregulated  
379 (**Figure 5B, left panel**). However, these genes did not appear to follow any functional pattern, and  
380 annotation enrichment analyses did not yield any significant results. In contrast, at 24 hpbf, and  
381 although the number of identified genes was smaller (109 downregulated, 71 over 2-fold; 13  
382 upregulated, 5 over 2-fold), most genes shown to date to be involved in systemic immune responses  
383 of the complement-like system and downstream effector reactions, including *TEP1*, *LRIM1*, *APLIC*  
384 and various clip-domain serine protease homologs, were downregulated (**Figure 5B, right panel**).  
385 Enrichment analysis confirmed that the serine protease/protease/hydrolase and the serine protease  
386 inhibitor/protease inhibitor protein classes were significantly overrepresented in this gene list. When  
387 considered together with the increased complement activity observed against  $\Delta c43$  compared to the  
388 *c507* ookinetes, these data could suggest induction of a negative feedback mechanism to  
389 downregulate this self-damaging innate immune response. However, most of these genes are  
390 thought to be largely, and in some cases exclusively, expressed in hemocytes and fat body cells;  
391 therefore, their detection as downregulated in midgut tissues cannot be easily explained. Thus, a  
392 more possible explanation is that midgut infection by  $\Delta c43$  ookinetes causes mobilization and  
393 differentiation of hemocytes attached to the midgut tissues as shown previously [28-30], causing a  
394 temporal depletion of relevant transcripts from the midgut tissue.

395 We examined this hypothesis by measuring the abundance of transcripts encoding the three major  
396 components of the complement-like system, *TEP1*, *LRIM1* and *APLIC*, in the midgut and whole  
397 body (excluding legs, wings and heads) of *A. coluzzii* mosquitoes infected with  $\Delta c43$  or control  
398 *c507* parasites at 24 hpbf. Since the  $\Delta c43$  phenotype was similar to the  $\Delta pbp47$  phenotype [16], and  
399 because unpublished data indicated similar *A. coluzzii* midgut responses to the two mutant parasite  
400 lines, transcript abundance in infections with  $\Delta pbp47$  parasites were also examined. The results  
401 revealed a striking difference in transcript abundance of all three genes between midgut and whole

402 mosquitoes (**Figure S7**). In accordance with the RNA sequencing data, the relative transcript  
403 abundance in infections with the two mutant parasite lines compared to control infections was lower  
404 in the midgut but higher in whole mosquitoes. These data corroborate our hypothesis that ookinetes  
405 lacking PIMMS43 or P47 trigger hemocyte mobilization and consequent depletion in the midgut  
406 tissue.

## 407 **Population genetics**

408 It has been shown that Pfs47 presents strong geographic structure in natural *P. falciparum*  
409 populations, both between continents and across Africa [31-33]. Furthermore, a small-scale  
410 genotypic analysis of oocysts sampled from *A. gambiae* and *A. funestus* mosquitoes in Tanzania  
411 revealed significant differentiation in Pfs47 haplotypes sampled from the two vectors [34]. These  
412 data are consistent with natural selection of Pfs47 haplotypes by the mosquito immune system and a  
413 key role of this interaction in parasite-mosquito coevolution [32]. However, a different study  
414 showed that polymorphisms in the *Pfs47* locus alone could not fully explain the observed variation  
415 in complement-mediated immune evasion of African *P. falciparum* strains [35].

416 We investigated the genetic structure of African *P. falciparum* populations with regards to  
417 *PfPIMMS43*, and compared this to the structure of *Pfs47*, using a rich dataset of 1,509 genome  
418 sequences of parasites sampled from 11 African countries in the context of the *P. falciparum*  
419 Community Project ([www.malariagen.net](http://www.malariagen.net)). The *PfPIMMS43* analysis revealed significant  
420 population differentiation as determined by the Fixation Index ( $F_{ST}$ ), mostly between populations of  
421 some West or Central (Democratic Republic of the Congo, DC) and East African countries  
422 ( $F_{ST}>0.1$ ; **Figure 6A**). The highest  $F_{ST}$  is detected in comparisons of Ugandan, DC or Kenyan  
423 populations with West African populations. The most differentiated SNPs are detected within the  
424 non-conserved region that is unique to *P. falciparum* (**Dataset S3**). Within this region, a SNP that  
425 leads to the non-synonymous substitution of Serine-217 to Leucine (S217L) is highly differentiated  
426 between sampled Kenyan/Tanzanian and all other populations, while a nearby SNP that leads to  
427 substitution of Glutamate-226 to Lysine (E225K) has swept to almost fixation in Ugandan  
428 populations.

429 The *PIMMS43*  $F_{ST}$  profile does not fully match the  $F_{ST}$  profile of *Pfs47* that also presents strong  
430 genetic differentiation between West and East Africa but is particularly strong for populations  
431 sampled in Madagascar and Malawi versus West African and DC populations (**Figure 6B**). The  
432 most highly differentiated SNPs are within domain 2 (D2) of the protein (**Dataset S3**). A SNP  
433 leading to substitution of Leucine-240 to Isoleucine (L240I) is almost fixed in Madagascar and  
434 Ugandan versus West African populations, while a nearby SNP leading to the non-synonymous  
435 substitution of Asparagine-271 to Isoleucine (N271I) is highly prevalent in DC versus all other  
436 populations, especially those sampled from East Africa. Our analysis also detected all four SNPs  
437 previously shown to differentiate between African (NF54) and New World (GB8) *P. falciparum*  
438 laboratory lines and lead to amino acid substitutions in the D2 region that contribute to immune  
439 evasion [36]; however, these SNPs were neither highly prevalent nor did they present significant  
440 geographic structure apart from that leading to Isoleucine-248 substitution to Leucine or Valine  
441 (I258L/V) that is significantly prevalent ( $F_{ST}>0.1$ ) in sampled Ugandan populations. These data  
442 concur with the hypothesis presented previously that polymorphisms in the D2 region of Pfs47,  
443 even those leading to synonymous substitutions, can alter the parasite immune evasion properties  
444 [36]. Finally, one of the substitutions defining the East versus West African differentiation is that of  
445 Glutamate-27 to Aspartate (E27D) at the start of the mature protein. This SNP is almost fixed in  
446 sampled Madagascar populations.

447 These data together reveal that *PfPIMMS43* and *Pfs47* exhibit significant geographic structure,  
448 consistent with their deduced role in parasite immune evasion. They also suggest that different  
449 selection pressures are exerted on each of these genes, which concurs with the hypothesis that the

450 two proteins serve different functions. A major difference between West and East African vector  
451 species is the presence of both *A. gambiae* (*A. gambiae* S-form) and *A. coluzzii* (*A. gambiae* M-  
452 form) in West Africa but only *A. gambiae* in East Africa. Interestingly, a resistant allele of *TEP1*,  
453 *TEP1<sup>rB</sup>*, is shown to have swept to almost fixation in West African *A. coluzzii* but be absent from *A.*  
454 *coluzzii* sampled from Cameroon, consistent with the high *PfPIMMS43 F<sub>ST</sub>* observed between  
455 Central and West African parasite populations, as well as from all sampled *A. gambiae* populations  
456 [37]. Therefore, it is tempting to speculate that a difference between West and East African vectors  
457 in their capacity to clear parasite infections through complement responses may have contributed to  
458 the observed *PfPIMMS43* and *Pfs47* genetic structure.

459 Moreover, *A. funestus* and *A. arabiensis* appear to have recently taken over from *A. gambiae* as the  
460 primary malaria vectors in many areas of East Africa [38], in contrast to West Africa where *A.*  
461 *gambiae* and *A. coluzzii* remain the primary vectors. Whilst nothing is known about the capacity of  
462 *A. funestus* to mount complement-like responses against malaria parasites, *A. arabiensis* is shown to  
463 be a less good vector of *P. berghei* but can be transformed into a highly susceptible vector, equal to  
464 *A. gambiae*, when its complement system is silenced [39]. Finally, *A. merus* is only found in coastal  
465 East Africa; although its abundance and contribution to malaria transmission has been increasing  
466 [40] it is unlikely that it has majorly contributed to structuring parasite populations.

#### 467 **Antibody-mediated transmission-blocking assays**

468 We examined in both *P. falciparum* and *P. berghei* whether targeting PIMMS43 using antibodies  
469 generated against each of the respective orthologous proteins could reduce parasite infectivity and  
470 malaria transmission potential. For *P. falciparum* transmission-blocking assays, purified IgG  $\alpha$ -  
471 Pfc43<sup>opt</sup> antibodies were added to gametocytemic blood at final concentrations of 0, 50, 125 and  
472 250  $\mu\text{g/mL}$  prior to offering this as bloodmeal to female *A. coluzzii* mosquitoes through optimized  
473 standard membrane feeding assays (SMFAs) [41]. Oocysts present in mosquito midguts at day-7  
474 post feeding were enumerated. The results showed strong inhibition of both infection intensity and  
475 infection prevalence in an antibody dose-dependent manner (**Figure 7A, Table S9**). At 125 and 250  
476  $\mu\text{g/mL}$  of antibody following four biological replicates, the overall inhibition of infection intensity  
477 observed was 57.1% and 76.2%, and the overall inhibition of infection prevalence was 37.3% and  
478 35.6%, respectively ( $P < 0.0001$ ).

479 Similar results were obtained with *P. berghei* transmission upon addition of  $\alpha$ -Pbc43<sup>S19</sup> antibodies  
480 to blood drawn from infected mice and provided to mosquitoes as bloodmeal in SMFAs.  
481 Statistically significant inhibition of both infection intensity and prevalence was detected at all  
482 antibody concentrations tested, i.e. 50, 100 and 250  $\mu\text{g/mL}$ , in an antibody dose-dependent manner  
483 (**Figure 7B, Table S10**). At 100  $\mu\text{g/mL}$ , the inhibition of oocyst intensity was 72.7% and the  
484 inhibition of infection prevalence was 35.5%, and these values increased to 90.3% and 65.6% at  
485 250  $\mu\text{g/mL}$ , respectively ( $P < 0.0001$ ).

486 A recent study has shown that antibodies binding a 52 amino acid region of Pfs47 confer strong  
487 transmission blocking of laboratory *P. falciparum* strains in *A. gambiae* [42]. In the same study,  
488 antibodies binding different regions of the protein showed either weak or no transmission blocking  
489 activity, consistent with an earlier study reporting that none of three monoclonal antibodies against  
490 Pfs47 could affect *P. falciparum* infections in *A. stephensi* [43]. These findings agree with the  
491 general understanding that antibodies binding different regions of a targeted protein can have  
492 profound differences in their blocking activity, especially when antibodies have a primarily  
493 neutralizing function [44, 45]. Indeed, our polyclonal  $\alpha$ -Pbc43<sup>opt</sup> antibody raised against codon-  
494 optimized PbPIMMS43 expressed in *E. coli* cells did not confer any transmission blocking activity  
495 against *P. berghei* (data not shown) despite producing strong signals in western blot analyses and  
496 immunofluorescence assays (see **Figures 1 and 2**). However, antibodies against fragments of

497 PSOP25 (synonym of PIMMS43) expressed in *E. coli* cells have been previously shown to inhibit  
498 *P. berghei* infection in *A. stephensi* [21, 46], albeit not as strongly as our  $\alpha$ -Pbc43<sup>Sf9</sup> antibodies.

## 499 **Concluding remarks and perspectives**

500 We demonstrate that PIMMS43 is required for parasite evasion of the mosquito immune response, a  
501 role also shared by P47 in both *P. falciparum* and *P. berghei* [14, 16]. The mechanism by which  
502 these molecules exert their function is unclear. A general explanation may lie with their GPI  
503 constituents or with their structural role in the formation of the ookinete sheath. On the one hand,  
504 *Plasmodium* GPIs are known to modulate the vertebrate host immune system [47], and studies have  
505 shown that mosquitoes mount a specific immune response against GPIs [48, 49]. On the other hand,  
506 the integrity of the ookinete sheath may be important for counteracting attacks by or acting as  
507 molecular sinks of free radicals produced during traversal of midgut epithelial cells [5, 6].  
508 Ookinetes lacking such membrane proteins may be unable to sustain these attacks and thus be  
509 irreversibly damaged and subsequently eliminated by the mosquito complement-like response. In  
510 relation to this, a specific function could be attributed to the conserved cysteine residues present in  
511 these proteins. Apart from their role in forming disulphide bridges thus serving a structural purpose,  
512 the ability of cysteine thiol groups to regulate the redox potential may be relevant [50].  
513 Interestingly, midgut infection with *P. berghei* is shown to inhibit the expression of catalase that  
514 mediates the removal of free radicals, and silencing catalase exacerbates ookinete elimination [51].  
515 Nonetheless, population genetic analyses indicate a more specific role of the two proteins in  
516 parasite-mosquito interactions and co-adaptation.

517 Notwithstanding their exact function in parasite immune evasion, PIMMS43, P47 and possibly  
518 other proteins involved in parasite immune evasion are good targets of interventions aiming to  
519 block malaria transmission in the mosquito. One such approach is transmission blocking vaccines  
520 (TBVs) aiming at generating antibodies in the human serum which, when ingested by mosquitoes  
521 together with gametocytes, interfere with the function of these proteins and block transmission to a  
522 new host [52]. Several putative TBVs are currently being investigated at a pre-clinical stage,  
523 including those targeting the gametocyte and/or ookinete proteins Pfs230, Pfs48/45 and Pfs25 [53].  
524 Another, more ambitious approach is the generation of genetically modified mosquitoes expressing  
525 single-chain antibodies or nanobodies which bind these proteins conferring refractoriness to  
526 infection and leading to malaria transmission blocking [54, 55]. Such genetic features can be spread  
527 within wild mosquito populations in a super-Mendelian fashion via means of gene drive (e.g.  
528 CRISPR/Cas9) and can lead to sustainable local malaria elimination [56].

529

## 530 **Materials and methods**

### 531 **Ethics statement**

532 All animal procedures were approved by the Imperial College Animal Welfare and Ethical Review  
533 Body (AWERB) and carried out in accordance with the Animal Scientific Procedures Act 1986  
534 under the UK Home Office Licenses PLL70/7185 and PPL70/8788.

### 535 **Sequence analysis**

536 *Plasmodium* DNA and protein sequences were retrieved from PlasmoDB  
537 (<http://plasmodb.org/plasmo/>). Protein sequences were aligned using ClustalW2 in the BioEdit  
538 sequence alignment editor program. Signal peptide and transmembrane domains were predicted  
539 using SignalP4.0 [57] and TMHMM Server v. 2.0 [58], respectively.



## 540 ***P. berghei* maintenance, culturing and purification**

541 The *P. berghei* ANKA lines used here include: *cl15cyl* (2.34), which is the reference parent line of  
542 *P. berghei* ANKA, *507m6c11* (*c507*) that constitutively expresses GFP integrated into the *230p* gene  
543 locus (*PBANKA\_0306000*) without a drug selectable marker [22]; *1804c11* (*c1804*) that  
544 constitutively expresses mCHERRY integrated into the *230p* locus without a drug selectable marker  
545 [23], and 2.33 [59] that is non-gametocyte producer and was used for asexual blood stage  
546 production. These lines were maintained in CD1 and/or Balb/c female mice (8-10 week old) by  
547 serial passage. Culturing and purification of *P. berghei* asexual blood stages, gametocytes and  
548 ookinetes were carried out as described [22].

## 549 ***P. falciparum* maintenance and culturing**

550 *P. falciparum* maintenance and culturing was performed as described [41]. Briefly, human red  
551 blood cells (hRBCs) were used for the maintenance of asexual blood stages and gametocyte culture  
552 of the *P. falciparum* NF54 strain. hRBCs of various blood groups were provided by the UK  
553 National Blood Service and used in the following order of preference: O+ male, O+ female, A+  
554 male and A+ female blood types. Donor blood was screened for human pathogens, aliquoted in 50  
555 mL Falcon tubes and centrifuged for the removal of serum and maintained at 4°C for up to two  
556 weeks post-delivery. *Pf*NF54 culture was maintained in complete medium (CM) composed of  
557 RPMI-1640-R5886 (Sigma), 0.05 g/L Hypoxanthine, 0.3 mg/L L-glutamine powder-(G8540-25G  
558 Sigma) and 10% sterile human serum of A+ serotype. Human serum was purchased from Interstate  
559 Blood Bank Inc., Memphis, Tennessee (no aspirin 2 hours prior to drawing, no anti-malarial  
560 treatment 2 weeks prior to drawing, and screened for common human pathogens). Quality control of  
561 the provided serum was tested by *in vitro* exflagellation test at days 14 and 16 post gametocyte  
562 induction. Set up of *Pf*NF54 asexual culture was performed in T25 cm<sup>2</sup> flasks containing a final  
563 volume of 500 µL of hRBCs (0.3-4% infection) and 10 mL of CM volume, kept at 37°C incubation  
564 and supplemented with “malaria gas” [3% O<sub>2</sub>/5% CO<sub>2</sub>/92% N<sub>2</sub> (BOC Special Gases, cat. no.  
565 226957-L-C)]. Gametocyte cultures were initiated by diluting the continuous sexual culture (3-4%  
566 ring forms) to 1% ring forms by the supply of fresh hRBCs. Gametocyte cultures were kept at  
567 constant temperature of 37°C until day 14 ensuring daily exchange of around 75% of the medium  
568 per flask. Parasitemia was assessed by Giemsa stained blood smears and gametocytemia and density  
569 of viable mature stage V gametocytes at day 14 post-induction were assessed by Giemsa stained  
570 blood smears and by testing *in vitro* exflagellation of male gametocytes respectively.

## 571 **Mosquito infections**

572 The mosquito strains used were N’gouso (*A. coluzzii*, previously M form *A. gambiae*) and SDA  
573 500 (*A. stephensi*). *P. berghei* mosquito infections were carried out by direct feeding of naïve or  
574 gene kd (see below) mosquitoes on mice with parasitaemia of 5-6% and gametocytaemia of 1-2%.  
575 Blood fed mosquitoes were maintained at 19-21°C, 70-80% humidity and 12/12 hours light/dark  
576 cycle. *P. berghei* mosquito infections were also carried out by standard membrane feeding as  
577 described below (*P. berghei* Standard Membrane Feeding Assay). *P. falciparum* mosquito  
578 infections were carried out by standard membrane feeding as described below (*P. falciparum*  
579 Standard Membrane Feeding Assay).

## 580 **RT-PCR and Quantitative RT-PCR**

581 Total RNA was extracted from parasites of *P. falciparum* NF54, *P. berghei* *c507*, *P. berghei*  $\Delta c43$   
582 and *P. berghei*<sup>*Pfc43*</sup>, and from naïve or *LRIMI* kd mosquitoes infected with either *P. falciparum*  
583 NF54, *P. berghei* *c507* and *P. berghei*  $\Delta c43$ , using TRIzol® reagent (ThermoFisher) according to  
584 the manufacturer’s instructions. Reverse transcription was performed on 2 µg of total RNA using

585 the Primescript Reverse Transcription Kit with a mixture of oligo-dT primers and random hexamers  
586 (Takara) after TURBO™ DNase (ThermoFisher) treatment. For RT-PCR, the resulting cDNA and  
587 gene specific RT-PCR primers were used in PCR of *P. falciparum* and *P. berghei* PIMMS43 (Table  
588 S11). Parasite stage specific control *P. falciparum* genes, *Pfs25* and *PfCSP*, and *P. berghei* genes,  
589 P28 and CTRP, and constitutively expressed *GFP* in *P. berghei* were also amplified using gene  
590 specific RT-PCR primers (Table S11). For qRT-PCR, SYBR green (Takara) and gene specific qRT-  
591 PCR primers (Table S11) were used according to the manufacturer's guidelines. Expression of  
592 *PbPIMMS43* was normalized against *GFP* and expression of *TEP1*, *LRIMI* and *APLIC* was  
593 normalized against *S7* using the  $\Delta\Delta Ct$  method.

#### 594 **Expression and purification of recombinant *P. falciparum* and *P. berghei* PIMMS43 in *E. coli***

595 *PfPIMMS43* and *PbPIMMS43* comprising the complete ORF was engineered (GeneArt,  
596 ThermoFisher) to contain codons allowing for optimal expression in *E. coli* and termed  
597 *PfPIMMS43<sup>opt</sup>/Pfc43<sup>opt</sup>* and *PbPIMMS43<sup>opt</sup>/Pbc43<sup>opt</sup>*, respectively. A *Pfc43<sup>opt</sup>* fragment encoding aa  
598 25-481 and a *Pbc43<sup>opt</sup>* fragment encoding aa 22-327 that both excludes the signal peptide and the C-  
599 terminal hydrophobic domain were amplified with primers containing overhangs for homology to  
600 the insertion vector and containing a NotI recognition site (Table S11). These fragments were  
601 cloned into a NotI digested protein expression vector plasmid, pET-32b (Novagen), using In-Fusion  
602 Cloning (Takara). Shuffle T7 *E. coli* cells (NEB) containing the recombinant protein expression  
603 plasmid were grown at 30°C and induced with 1 mM isopropyl-1-thio- $\beta$ -d-galactopyranoside at  
604 19°C for 16 h. Cells were harvested by centrifugation and lysed using bugbuster-lysonase  
605 (Novagen) containing Protease Inhibitors (cOmplete EDTA-free, Roche). Cell debris were removed  
606 by centrifugation. Both proteins were expressed as a 6xHistidine and thioredoxin tagged versions.  
607 The *Pfc43<sup>opt</sup>* recombinant protein was soluble and purified by cobalt affinity chromatography using  
608 TALON® metal affinity resin (Takara) under native conditions in phosphate buffered saline (PBS),  
609 pH 7.4. The *Pbc43<sup>opt</sup>* recombinant protein was extracted from inclusion bodies using the Inclusion  
610 Body Solubilization Reagent (ThermoFisher). The solubilized protein was also purified using  
611 TALON® metal affinity resin, however under denaturing conditions in 8M urea in PBS, pH 7.4.  
612 Refolding of *Pbc43<sup>opt</sup>* was carried out in decreasing concentrations of urea in PBS. Protein samples  
613 were analyzed by SDS-PAGE to determine purity prior to their use for immunization in rabbits for  
614 the generation of the polyclonal antibodies  $\alpha$ -*Pfc43<sup>opt</sup>* and  $\alpha$ -*Pbc43<sup>opt</sup>*.

#### 615 **Expression and purification of recombinant *P. berghei* PIMMS43 in Sf9 Insect cells**

616 A 930 bp fragment of endogenous *PbPIMMS43* encoding aa 22-331 that excludes the signal peptide  
617 and includes four amino acids of the C-terminal hydrophobic domain was amplified from cDNA  
618 prepared from 24 h *in vitro* ookinetes with primers containing overhangs for homology to the  
619 insertion vector (Table S11). This fragment was cloned by ligation independent cloning into the  
620 linearized pIEX-10 EK-LIC vector which carries a C-terminal 10xHis tag (Novagen) to generate  
621 pIEX-10: *Pbc43*-SP/TM. A stable line expressing the recombinant protein was generated by co-  
622 transfection of pIEX-10: *Pbc43*-SP/TM and pIEX-10:Neo plasmid [11] using the Cellfectin® II  
623 Reagent (ThermoFisher) according to the manufacturers' guidelines. pIEX-10:Neo plasmid carries  
624 the neomycin resistance cassette and provides resistance to the antibiotic G418 (Sigma) which  
625 allows for selection of transfected cells. Stable cell lines expressing the recombinant protein were  
626 initially maintained in complete medium comprising of serum free medium Sf-900 II SFM  
627 (ThermoFisher) complemented with 10% v/v foetal bovine serum (Sigma), weaned of FBS and  
628 maintained only in serum free media. The recombinant protein was extracted from cells using lysis  
629 buffer (1XPBS, 1% v/v Triton X-100, pH 7.4) containing benzonase (Novagen) and Protease  
630 Inhibitors (cOmplete EDTA-free, Roche). The His-tagged recombinant *PbPIMMS43* protein was  
631 insoluble and extracted by solubilization in 8M urea in PBS, pH 7.4. The protein was purified using

632 TALON® metal affinity resin under denaturing conditions in 8M urea in PBS, pH 7.4. Bound  
633 proteins were eluted using denaturing elution buffer. Refolding of Pbc43 was carried out in  
634 decreasing concentrations of urea in PBS. Protein samples were analyzed by SDS-PAGE to  
635 determine purity prior to their use for immunization in rabbits in the generation of the polyclonal  
636 antibody  $\alpha$ -Pbc43 for use in transmission blocking assays.

### 637 **Antibody production**

638 We generated a rabbit polyclonal antibody against PfPIMMS43 targeting a codon-optimized region  
639 (25-481 amino acids) expressed in *E. coli*. Two rabbit polyclonal antibodies were generated against  
640 PbPIMMS43. The first ( $\alpha$ -Pbc43<sup>Sf9</sup>) was raised against the 22-331 amino acid fragment expressed  
641 in Sf9 insect cell line and the second ( $\alpha$ -Pbc43<sup>opt</sup>) was raised the 22-327 codon-optimized amino  
642 acid fragment expressed in *E. coli*. All polyclonal antibodies were purified from pooled sera of two  
643 immunized rabbits (Eurogentec).

### 644 **Western blot analysis**

645 Whole cell lysates were prepared by suspending purified parasite pellets in whole cell lysis buffer  
646 (1XPBS, 1% v/v Triton X-100) containing Protease Inhibitors (cOmplete EDTA-free, Roche). 24 h  
647 *in vitro* ookinetes were also subjected to cellular fractionation using the following method. 24 h *in*  
648 *vitro* ookinetes were resuspended in soluble lysis buffer (5 mM Tris-HCl, pH 7.4) containing  
649 Protease Inhibitors. This sample underwent two freeze thaw cycles by incubating at -80°C for 6 h  
650 and thawing at 30°C for 15 min. Cell lysate was centrifuged to obtain the soluble fraction. The  
651 pellet was resuspended in membrane lysis buffer (50 mM Tris-HCl, 150 mM NaCl, 1% v/v Triton  
652 X-100, pH 7.4), incubated on ice for 30 min and centrifuged to obtain the Triton soluble fraction.  
653 The pellet was resuspended for a last time in Laemilli buffer (+/- 3-5% v/v 2-mercapthoethanol),  
654 boiled at 95°C for 10 min and centrifuged to obtain the insoluble fraction. Protein samples were  
655 then boiled under non-reducing or reducing (+ 3-5% v/v 2-mercapthoethanol) conditions in  
656 Laemilli buffer and separated using 10% sodium dodecyl sulfate polyacrylamide gel  
657 electrophoresis. Separated proteins were then transferred to a PVDF membrane (GE Healthcare).  
658 Proteins were detected using  $\alpha$ -Pbc43<sup>opt</sup> (1:100),  $\alpha$ -Pfc43<sup>opt</sup> (1:100), goat  $\alpha$ -GFP (Rockland  
659 chemicals) (1:100) and 13.1 mouse monoclonal  $\alpha$ -P28 [60] (1:1000) antibodies. Secondary  
660 horseradish peroxidase (HRP) conjugated goat  $\alpha$ -rabbit IgG, goat  $\alpha$ -mouse IgG antibodies  
661 (Promega) and donkey  $\alpha$ -goat IgG (Abcam) were used at 1: 10,000, 1: 10,000 and 1: 5,000  
662 dilutions, respectively. All primary and secondary antibodies were diluted in 3% milk-PBS-Tween  
663 (0.05% v/v) blocking buffer.

### 664 **Indirect immunofluorescence assay**

665 IFA's were carried out on *P. falciparum* and *P. berghei* mosquito stages and include blood bolus  
666 parasites at 1 hpb, ookinetes invading the midgut epithelium at 24-30 hpb, oocysts at 2 dpb, *P.*  
667 *falciparum* and *P. berghei* oocyst sporozoites at 9-11 and 14-16 dpb respectively, and *P.*  
668 *falciparum* and *P. berghei* salivary gland sporozoites at 16 and 21 dpb respectively. For IFA's on  
669 blood bolus parasites, midguts of blood fed mosquitoes were dissected, and the blood boluses were  
670 collected. Blood bolus was washed in PBS prior to fixation in 4% paraformaldehyde (PFA) in PBS  
671 for 30 min. Fixed parasites were smeared on glass slides, allowed to air dry, permeabilized with  
672 0.2% v/v Triton X-100, and blocked in a 3% w/v bovine serum albumin (all diluted in PBS). For  
673 IFA's on ookinetes invading the midgut epithelium or young oocysts, midguts of blood fed  
674 mosquitoes were dissected, and blood boluses were discarded. The midgut epithelium was fixed in  
675 4% PFA in PBS for 45 min and washed thrice in PBS for 10 min each. Midgut epithelium was  
676 permeabilized and blocked for 1 h with 1% w/v BSA, 0.1% v/v Triton X-100 in PBS. For IFA's on  
677 sporozoites, infected midguts and salivary glands were dissected, and tissues were homogenized to

678 release sporozoites. Sporozoites were fixed, blocked and permeabilized as that used for blood bolus  
679 parasites. Samples were then stained in blocking solution with primary antibodies ( $\alpha$ -Pfc43<sup>opt</sup>,  
680 1:300; 4B7 mouse monoclonal  $\alpha$ -Pfs25 [61], 1:1000; 2A10 mouse monoclonal  $\alpha$ -PfCSP [62],  
681 1:200;  $\alpha$ -Pbc43<sup>opt</sup>, 1:100; 13.1 mouse monoclonal  $\alpha$ -P28, 1:1000, 3D11 mouse monoclonal  $\alpha$ -  
682 PbCSP [63], 1:100; and rabbit  $\alpha$ -TEP1 [10], 1:300. Alexa Fluor (488 and 568) conjugated  
683 secondary goat antibodies specific to rabbit or mouse (ThermoFisher) were used at a dilution of  
684 1:1000. 4',6-diamidino-2-phenylindole (DAPI) was used to stain nuclear DNA. Images were  
685 acquired using a Leica SP5 MP confocal laser-scanning microscope. Images underwent processing  
686 by deconvolution using Huygens software and were visualized using Image J.

## 687 **Generation of transgenic parasites**

688 Partial ko of *P. berghei* *c43* CDS was carried out by double crossover homologous recombination  
689 in the *c507* and *1804c11* lines. For partial disruption in the *c507* line, a 765 bp upstream homology  
690 region in the *PbPIMMS43* 5'UTR was amplified from *P. berghei* 2.34 genomic DNA as an ApaI  
691 and HindIII fragment using primers P1 and P2 respectively. A 528 bp downstream homology region  
692 in the most 3' region of the CDS was amplified as an EcoRI and BamHI fragment using primers P3  
693 and P4 respectively. These fragments were cloned into the pBS-TgDHFR vector which carries a  
694 modified *Toxoplasma gondii* dihydrofolate gene (*TgDHFR/TS*) cassette that confers resistance to  
695 pyrimethamine [64]. The targeting cassette was released by ApaI/BamHI digestion and it allows ko  
696 of 50% of *P. berghei* *c43* CDS at the 5' region. For partial disruption in the *1804c11* line, the target  
697 vector containing the human *DHFR* selection cassette was used (kindly provided by plasmogEM,  
698 vector design ID, PbGEM-042760; <http://plasmogem.sanger.ac.uk/>). *hDHFR* confers resistance to  
699 the drugs pyrimethamine and WR92210. The targeting cassette was released by NotI digestion and  
700 allows ko of 74% of *PbPIMMS43* CDS leaving a small part of the 3' region of the CDS.

701 To express *P. falciparum* *c43* in *P. berghei*, the transgenic parasite *Pb<sup>Pfc43</sup>* was created in the *c507*  
702 line. The *Pfc43* replacement construct was generated using the plasmid pL0035 which carries the  
703 *hDHFR* selection cassette [65]. Upstream of the selectable marker cassette, a 1.7 kb fragment  
704 upstream of the *PbPIMMS43* ATG start codon was amplified using the HindIII and ApaI primer  
705 pair P12 and P13 respectively. The 1.5 kb *Pfc43* coding DNA sequence was amplified from cDNA  
706 using the ApaI and SacII primer pair P14 and P15 respectively. A 518 bp region corresponding to  
707 the 3'UTR, downstream of the *PbPIMMS43* stop codon, was amplified as a SacII fragment using  
708 primers P16 and P17. Downstream of the selectable marker, a 700 bp region corresponding to part  
709 of the *PbPIMMS43* coding region and part of the 3'UTR was amplified as a XhoI and SmaI  
710 fragment using primers P18 and P19 respectively. These fragments were cloned into pL0035 and  
711 the targeting cassette was released by HindIII and SmaI digestion.

712 To re-introduce *PbPIMMS43* into the  $\Delta c43$  ko parasite, the transgenic parasite  $\Delta c43::c43^{wt}$  was  
713 created. A 3.5 kb upstream region that includes the *PbPIMMS43* ORF and its 5'UTR and 3'UTR  
714 was amplified as a HindIII and SacII fragment using primers P22 and P23 respectively. A 518 bp  
715 downstream region corresponding to the *PbPIMMS43* 3'UTR was amplified as a XhoI and SmaI  
716 fragment using primers P24 and P25, respectively. These fragments were cloned into the pL0035  
717 vector and served as homology regions for homologous recombination at the  $\Delta c43$  ko locus in the  
718 *c507* line. The targeting cassette was released by HindIII and SmaI digestion.

719 Transfection of linearized constructs, selection of transgenic parasites and clonal selection was  
720 carried out as described previously [22].

## 721 **Genotypic analysis of transgenic parasites**

722 Purified blood stage parasites were obtained after white blood cells removal using hand packed  
723 cellulose (Sigma) columns and red blood cell lysis in 0.17M NH<sub>4</sub>Cl on ice for 20 min. Genomic



724 DNA was extracted from parasites using the DNeasy kit (Qiagen). Detection of successful  
725 integration events or maintenance of the unmodified locus was performed by PCR on genomic  
726 DNA using primers listed in Table S11. Blood stage parasites within agarose plugs were lysed in  
727 lysis buffer (1XTNE, 0.1 M EDTA pH 8.0, 2% (v/v) Sarkosyl, 400µg/mL proteinase K) to release  
728 nuclear chromosomes. Southern blot analysis on pulsed field gel electrophoresis separated  
729 chromosomes (Run settings: 98 volts, 1-5 mins pulse time for 60 h at 14 °C) was carried out with a  
730 probe targeting the *TgDHFR/TS-P. berghei DHFR 3'UTR*, obtained by HindIII and EcoRV  
731 digestion of the pBS-TgDHFR plasmid.

### 732 **Exflagellation assays**

733 Exflagellation assays were performed by adding tail blood from a high gametocytemia mouse to  
734 ookinete medium (RPMI 1640, 20% v/v FBS, 100 µM xanthurenic acid, pH 7.4) in a 1:40 ratio.  
735 Following a 10 min incubation at RT, exflagellation was observed and counted in a standard  
736 haemocytometer at 40X magnification using a light microscope. Exflagellation was compared to the  
737 male gametocytaemia determined from Giemsa stained blood smears.

### 738 **Macrogamete to ookinete conversion assays**

739 For *in vitro* assays, 100 µL of a 24 h *in vitro* ookinete culture was pelleted, washed in PBS and  
740 resuspended in the same volume of fresh ookinete media. For *in vivo* assays, the blood bolus of 10  
741 mosquitoes at 17-18 hpbf was pelleted, washed in PBS and resuspended in 50 µL of fresh ookinete  
742 media. The suspension was then incubated with a Cy3-labelled 13.1 mouse monoclonal α-P28 (1:50  
743 dilution) for 20 min on ice. The α-P28 antibody was conjugated with the Cy3 fluorescent dye using  
744 the Cy®3 Ab Kit GE Healthcare (Sigma-Aldrich) according to the manufacturer's instructions. The  
745 conversion rate was calculated as the percentage of Cy3 positive ookinetes to Cy3 positive  
746 macrogametes and ookinetes.

### 747 **Ookinete motility assays**

748 Ookinete motility assays were performed as previously described [66]. Briefly, 24 h *in vitro*  
749 ookinete culture was added to Matrigel (BD biosciences) on ice in a 1:1 ratio, mixed thoroughly,  
750 dropped onto a slide, covered with a Vaseline rimmed cover slip, and sealed with nail varnish. The  
751 Matrigel-ookinete mixture was let to set at RT for 30 min. Time-lapse microscopy (1 frame every 5  
752 seconds, for 10 min) of ookinetes were taken using the differential interference contrast (DIC)  
753 settings with a 40X objective lens on a Leica DMR fluorescence microscope and a Zeiss AxioCam  
754 HRc camera controlled by the Axiovision (Zeiss) software. The speed of individual ookinetes was  
755 measured using the manual tracking plugin in the Icy software package  
756 (<http://icy.bioimageanalysis.org/>).

### 757 **Gene silencing in *A. coluzzii***

758 cDNA was prepared from total RNA extracted (as described above) from *A. coluzzii* midgut  
759 infected with *P. berghei c507*, at 24 hpbf. The cDNA was used in the amplification of *CTL4*, *LRIMI*  
760 and *TEPI* using primers with T7 overhangs as reported in [67, 68]. The resulting T7 PCR products  
761 and the T7 high yield transcription kit (ThermoFisher) was used to produce dsRNA. DsRNA was  
762 purified using the RNeasy kit (Qiagen) and 0.2 µg in 69 nL was injected into the thorax of *A.*  
763 *coluzzii* mosquitoes using glass capillary needles and the Nanoject II microinjector (Drummond  
764 Scientific). Injected mosquitoes were left for 2-3 days before *P. berghei* infection.

## 765 **Ookinete invasion assay**

766 *CTL4* kd *A. coluzzii* mosquitoes were infected with *c507 wt* or  $\Delta c43$  parasite lines by direct feeding.  
767 At 4 dpbf, following midgut dissection, melanized parasites were visualized under the light  
768 microscope and counted.

## 769 **Ookinete injections in mosquito haemocoel**

770 24 h *in vitro* ookinetes was adjusted with RPMI 1640 to achieve an injection concentration of 800  
771 ookinetes per mosquito as described previously [69]. This was injected into the thorax of *A. coluzzii*  
772 mosquitoes using glass capillary needles and the Nanoject II microinjector. Salivary gland  
773 sporozoites were counted at 21 dpbf.

## 774 **Imaging and enumeration of parasites**

775 Following dissection, infected midguts tissues were fixed in 4% PFA in PBS for 20 min at room  
776 temperature and washed twice for 5 min each in PBS. Fixed midguts were mounted in  
777 Vectashield® (VectorLabs) and oocysts or melanised ookinetes were enumerated using light and/or  
778 fluorescence microscopy. Oocyst images and sizes were also analyzed using fluorescence  
779 microscopy. Oocyst and salivary gland sporozoite numbers at 15 and 21 dpbf respectively were  
780 counted using a standard haemocytometer, in 3 technical replicates of homogenates of 10 *P. berghei*  
781 infected *A. coluzzii* midguts or salivary glands.

## 782 **Mosquito to mouse transmission**

783 For each independent experiment, at least 30 *P. berghei* infected mosquitoes were allowed to feed  
784 on 2-3 anaesthetized C57/BL6 mice at 20-22 dpbf. Parasitaemia was monitored up until 14 days  
785 post mosquito bite by Giemsa stained tail blood smears.

## 786 **RNA-sequencing library preparation**

787 Three replicate infections of *A. coluzzii* mosquitoes with the  $\Delta c43$  and *c507 P. berghei* lines were  
788 performed and infected midguts were dissected at 1 and 24 hpbpf. Total RNA was extracted as  
789 described elsewhere and was used for RNA sequencing by Genewiz (New Jersey, US) using the  
790 NEB Ultra prep kit and an Illumina HiSeq platform with 150x2 paired-end reads. Prior to the RNA  
791 sequencing, successful infection of the midgut epithelium was confirmed by P28-staining of  
792 parasites in 5 midguts from each replicate infection: Replicate 1, *c507* median 536 (458, 635, 495,  
793 536, 598),  $\Delta c43$  median 501 (419, 436, 501, 605, 520), Replicate 2, *c507* median 386 (386, 421,  
794 350, 258, 408),  $\Delta c43$  median 389 (347, 411, 389, 369, 402) and Replicate 3, *c507* median 548 (501,  
795 426, 548, 603, 551),  $\Delta c43$  median 495 (495, 504, 521, 465, 436).

## 796 **NGS RNA-sequencing-Data processing and analysis**

797 RNA-Seq reads were mapped using HiSat2 v2.0.5 [70] with default parameters to the *A. gambiae*  
798 genome (AgamP4 assembly) [71] and the *P. berghei ANKA* [72]. Transcript abundance was  
799 quantified as fragments per kilobase per million reads (FPKM) using Cufflinks v2.2.1 [73] on the *A.*  
800 *gambiae* (Anopheles-gambiae-PEST\_BASEFEATURES\_AgamP4.9.gtf) and *P. berghei*  
801 (PlasmoDB-39\_PbergheiANKA.gff) annotation sets. Differential expression analysis was  
802 performed using Cuffdiff v.2.2.1 [74]. The sequencing data were uploaded to the Galaxy web  
803 platform (an open source, web-based platform for data intensive biomedical research), and we used  
804 the VectorBase Galaxy server (<https://galaxy.vectorbase.org>) to analyze the data [75]. Data are  
805 derived from three independent biological replicates, each of which included three technical  
806 replicates. To filter out the biological or technical noise from the actively expressed genes, an

807 FPKM cutoff was selected that is based on an implementation of the zFPKM normalization method  
808 described previously [76]. Functional classification of *P. berghei* differential regulated genes were  
809 performed in PlasmoDB (<http://plasmodb.org/plasmo/>) using the *P. berghei* full genome as a  
810 reference genome. PANTHER (v13.1; <http://pantherdb.org>) [77] was used for functional  
811 classification of *A. gambiae* differentially regulated genes. The RNA sequencing data were  
812 deposited to and can be downloaded from the European Nucleotide Archive with experiment codes  
813 ERX3197375-410.

## 814 **Population genetics analysis**

815 The genome sequences of 1,509 African *P. falciparum* samples determined in the context of the *P.*  
816 *falciparum* Community Project were obtained from the MalariaGen website  
817 (<http://www.malariagen.net/data>). They include samples from 11 African countries including  
818 Gambia (73), Guinea (124), Mali (87), Burkina Faso (56), Ghana (478), DR of the Congo (279),  
819 Uganda (12), Kenya (52), Tanzania (68), Malawi (262) and Madagascar (18). Call of SNPs found in  
820 *PfPIMMS43* and *Pfs47* exonic sequences were based on the 3D7 reference genome assembly  
821 version 6.0 (Jan. 2016).  $F_{ST}$  values were calculated using the R (v.3.2.1) packages *gdsfmt* and  
822 *SNPRelate* [78] by considering (a) all SNPs across each gene and all populations within a given  
823 country and (b) each individual SNP sampled from populations in each of the 11 African countries  
824 ( $F_{ST}$  total) and in pairwise country comparisons.

## 825 ***P. falciparum* standard membrane feeding assays (SMFAs)**

826 SMFA was carried out as described previously [41]. Briefly, day 14, stage V gametocytes cultures  
827 were pooled in a pre-warmed tube containing 20% v/v uninfected serum-free hRBCs and 50% v/v  
828 heat-inactivated human serum. The  $\alpha$ -Pfc43<sup>opt</sup> antibodies were added to the gametocytemic blood  
829 mix in pre-warmed Eppendorf tubes to final antibody concentrations of 50, 125 and 250  $\mu$ g/mL, in  
830 a final volume of 300  $\mu$ L. This was immediately transferred to pre-warmed glass feeders kept a  
831 constant temperature of 37°C. A negative control mix containing no  $\alpha$ -Pfc43<sup>opt</sup> antibodies was also  
832 set up. Blood fed mosquitoes were maintained at 27°C, 70% humidity and 12/12 hours light/dark  
833 cycle. On 7 dpbf, midguts were dissected as described above and infection intensity and prevalence  
834 recorded using light microscopy.

## 835 ***P. berghei* SMFAs**

836 SMFA was carried out as described previously [79]. Briefly, female *An. stephensi* mosquitoes were  
837 starved for 24 h prior to feeding on *P. berghei* infected blood. For each feed, 350  $\mu$ L of heparanized  
838 *P. berghei* ANKA 2.34 infected blood containing asexual parasite and gametocyte stages with a  
839 parasitaemia of 5-6% and gametocytaemia of 2-3% was mixed with 150  $\mu$ L of PBS containing  
840 either  $\alpha$ -Pbc43 or the isotopic monoclonal UPC10 (negative control) (Sigma) antibodies to yield  
841 final antibody concentrations of 50, 100 and 250  $\mu$ g/mL. Blood fed mosquitoes were maintained as  
842 described above. On 10 dpbf, mosquito midguts were dissected as described above and oocyst  
843 intensity and prevalence were recorded.

## 844 **Statistical analysis**

845 Statistical analysis for exflagellation, ookinete conversion, motility assays and TEPI ookinete  
846 binding was performed using a two-tailed, unpaired Student's *t*-test. For statistical analyses of the  
847 oocyst or melanized parasite load (infection intensity) and presence of oocysts (infection  
848 prevalence), *p* values were calculated using the Mann-Whitney test and the Fishers exact test,  
849 respectively. Statistical analyses were performed using GraphPad Prism v7.0. The generalized  
850 linear mixed model (GLMM) was used to also determine statistical significance in oocyst infection

851 intensity in transmission blocking assays. GLMM analyses were performed in R (version 2.15.3)  
852 using the Wald Z-test on a zero-inflated negative binomial regression (glmmADMB). The various  
853 treatments were considered as covariates and the replicates as a random component. Fixed effect  
854 estimates are the regression coefficients.

855

## 856 **Acknowledgments**

857 The work was funded by a Wellcome Trust Investigator Award (107983/Z/15/Z) to G.K.C., a  
858 Wellcome Trust Project grant (093587/Z/10/Z) to G.K.C. and D.V., and a Bill and Melinda Gates  
859 Foundation grant (OPP1158151) to G.K.C. L.D.P.R. was funded by a Royal Society Newton  
860 International Fellowship (NF161472). A.M.B. was funded by a Medical Research Council New  
861 Investigator grant (MR/N00227X/1). The authors thank Ana-Rita Gomes for assistance with  
862 transfection and cloning of the  $\Delta c43^{red}$  parasite line and Melina Campos for assistance with GLMM  
863 analysis, and Katarzyna Sala, Chrysanthi Taxiarchi, Lara Selles, and Neil Mac Aogain for technical  
864 assistance. The paper is dedicated to the memory of Hassan Yassine who carried out initial work.

865

## 866 **Author Contributions**

867 Conceptualization, G.K.C. and D.V.; Methodology, C.V.U., M.G., L.D.P.R., G.K.C. and D.V.;  
868 Validation, M.G. and C.W.; Formal analysis, C.V.U., M.G., L.D.P.R., G.K.C. and D.V.;  
869 Investigation, C.V.U., M.G., S.T., F.A., A.M.B.; Resources, G.K.C. and D.V.; Data Curation, A.J.  
870 and D.V.; Writing Original Draft, C.V.U., M.G., G.K.C. and D.V.; Writing Paper, G.K.C. and D.V.;  
871 Visualization, G.K.C. and D.V.; Supervision, G.K.C. and D.V.; Project Administration, G.K.C. and  
872 D.V.; Funding Acquisition, G.K.C. and D.V.

873

## 874 **References**

- 875 1. Clayton AM, Dong Y, Dimopoulos G. The Anopheles Innate Immune System in the  
876 Defense against Malaria Infection. *J Innate Immun.* 2014;6(2):169-81. Epub 2013/08/31. doi:  
877 10.1159/000353602. PubMed PMID: 23988482.
- 878 2. Povelones M, Osta MA, Christophides GK. The Complement System of Malaria Vector  
879 Mosquitoes. *Adv Insect Physiol.* 2016;51:223-42. doi: 10.1016/bs.aiip.2016.06.001. PubMed  
880 PMID: WOS:000383859500009.
- 881 3. Alavi Y, Arai M, Mendoza J, Tufet-Bayona M, Sinha R, Fowler K, et al. The dynamics of  
882 interactions between Plasmodium and the mosquito: a study of the infectivity of Plasmodium  
883 berghei and Plasmodium gallinaceum, and their transmission by Anopheles stephensi, Anopheles  
884 gambiae and Aedes aegypti. *Int J Parasitol.* 2003;33(9):933-43. Epub 2003/08/09. PubMed PMID:  
885 12906877.
- 886 4. Smith RC, Vega-Rodriguez J, Jacobs-Lorena M. The Plasmodium bottleneck: malaria  
887 parasite losses in the mosquito vector. *Mem Inst Oswaldo Cruz.* 2014;109(5):644-61. PubMed  
888 PMID: 25185005; PubMed Central PMCID: PMC4156458.
- 889 5. Garver LS, de Almeida Oliveira G, Barillas-Mury C. The JNK pathway is a key mediator of  
890 Anopheles gambiae antiplasmodial immunity. *PLoS Pathog.* 2013;9(9):e1003622. doi:



- 891 10.1371/journal.ppat.1003622. PubMed PMID: 24039583; PubMed Central PMCID:  
892 PMCPMC3764222.
- 893 6. Oliveira Gde A, Lieberman J, Barillas-Mury C. Epithelial nitration by a peroxidase/NOX5  
894 system mediates mosquito antiplasmodial immunity. *Science*. 2012;335(6070):856-9. doi:  
895 10.1126/science.1209678. PubMed PMID: 22282475; PubMed Central PMCID:  
896 PMCPMC3444286.
- 897 7. Blandin S, Shiao SH, Moita LF, Janse CJ, Waters AP, Kafatos FC, et al. Complement-like  
898 protein TEP1 is a determinant of vectorial capacity in the malaria vector *Anopheles gambiae*. *Cell*.  
899 2004;116(5):661-70. PubMed PMID: 15006349.
- 900 8. Levashina EA, Moita LF, Blandin S, Vriend G, Lagueux M, Kafatos FC. Conserved role of  
901 a complement-like protein in phagocytosis revealed by dsRNA knockout in cultured cells of the  
902 mosquito, *Anopheles gambiae*. *Cell*. 2001;104(5):709-18. PubMed PMID: 11257225.
- 903 9. Fraiture M, Baxter RH, Steinert S, Chelliah Y, Frolet C, Quispe-Tintaya W, et al. Two  
904 mosquito LRR proteins function as complement control factors in the TEP1-mediated killing of  
905 *Plasmodium*. *Cell Host Microbe*. 2009;5(3):273-84. doi: 10.1016/j.chom.2009.01.005. PubMed  
906 PMID: 19286136.
- 907 10. Povelones M, Waterhouse RM, Kafatos FC, Christophides GK. Leucine-rich repeat protein  
908 complex activates mosquito complement in defense against *Plasmodium* parasites. *Science*.  
909 2009;324(5924):258-61. Epub 2009/03/07. doi: 10.1126/science.1171400. PubMed PMID:  
910 19264986; PubMed Central PMCID: PMC2790318.
- 911 11. Povelones M, Bhagavatula L, Yassine H, Tan LA, Upton LM, Osta MA, et al. The CLIP-  
912 domain serine protease homolog SPCLIP1 regulates complement recruitment to microbial surfaces  
913 in the malaria mosquito *Anopheles gambiae*. *PLoS Pathog*. 2013;9(9):e1003623. doi:  
914 10.1371/journal.ppat.1003623. PubMed PMID: 24039584; PubMed Central PMCID:  
915 PMCPMC3764210.
- 916 12. Yassine H, Kamareddine L, Chamat S, Christophides GK, Osta MA. A serine protease  
917 homolog negatively regulates TEP1 consumption in systemic infections of the malaria vector  
918 *Anopheles gambiae*. *J Innate Immun*. 2014;6(6):806-18. Epub 2014/07/12. doi:  
919 10.1159/000363296. PubMed PMID: 25012124; PubMed Central PMCID: PMCPMC4813755.
- 920 13. Schlegelmilch T, Vlachou D. Cell biological analysis of mosquito midgut invasion: the  
921 defensive role of the actin-based ookinete hood. *Pathog Glob Health*. 2013;107(8):480-92. Epub  
922 2014/01/17. doi: 10.1179/2047772413Z.000000000180. PubMed PMID: 24428832; PubMed  
923 Central PMCID: PMCPMC4073529.
- 924 14. Molina-Cruz A, Garver LS, Alabaster A, Bangiolo L, Haile A, Winikor J, et al. The human  
925 malaria parasite *Pfs47* gene mediates evasion of the mosquito immune system. *Science*.  
926 2013;340(6135):984-7. Epub 2013/05/11. doi: 10.1126/science.1235264. PubMed PMID:  
927 23661646; PubMed Central PMCID: PMC3807741.
- 928 15. Ramphul UN, Garver LS, Molina-Cruz A, Canepa GE, Barillas-Mury C. *Plasmodium*  
929 *falciparum* evades mosquito immunity by disrupting JNK-mediated apoptosis of invaded midgut  
930 cells. *Proc Natl Acad Sci U S A*. 2015;112(5):1273-80. doi: 10.1073/pnas.1423586112. PubMed  
931 PMID: 25552553; PubMed Central PMCID: PMCPMC4321252.
- 932 16. Ukegbu CV, Giorgalli M, Yassine H, Ramirez JL, Taxiarchi C, Barillas-Mury C, et al.  
933 *Plasmodium berghei* P47 is essential for ookinete protection from the *Anopheles gambiae*  
934 complement-like response. *Sci Rep*. 2017;7(1):6026. Epub 2017/07/22. doi: 10.1038/s41598-017-  
935 05917-6. PubMed PMID: 28729672; PubMed Central PMCID: PMCPMC5519742.

- 936 17. van Dijk MR, van Schaijk BC, Khan SM, van Dooren MW, Ramesar J, Kaczanowski S, et  
937 al. Three members of the 6-cys protein family of *Plasmodium* play a role in gamete fertility. *PLoS*  
938 *Pathog.* 2010;6(4):e1000853. doi: 10.1371/journal.ppat.1000853. PubMed PMID: 20386715;  
939 PubMed Central PMCID: PMCPMC2851734.
- 940 18. Akinosoglou KA, Bushell ES, Ukegbu CV, Schlegelmilch T, Cho JS, Redmond S, et al.  
941 Characterization of *Plasmodium* developmental transcriptomes in *Anopheles gambiae* midgut  
942 reveals novel regulators of malaria transmission. *Cell Microbiol.* 2015;17(2):254-68. doi:  
943 10.1111/cmi.12363. PubMed PMID: 25225164; PubMed Central PMCID: PMCPMC4371638.
- 944 19. Ukegbu CV, Akinosoglou KA, Christophides GK, Vlachou D. *Plasmodium berghei*  
945 PIMMS2 promotes ookinete invasion of the *Anopheles gambiae* mosquito midgut. *Infect Immun.*  
946 2017. Epub 2017/06/01. doi: 10.1128/IAI.00139-17. PubMed PMID: 28559405; PubMed Central  
947 PMCID: PMCPMC5520436.
- 948 20. Kaneko I, Iwanaga S, Kato T, Kobayashi I, Yuda M. Genome-Wide Identification of the  
949 Target Genes of AP2-O, a *Plasmodium* AP2-Family Transcription Factor. *PLoS Pathog.*  
950 2015;11(5):e1004905. Epub 2015/05/29. doi: 10.1371/journal.ppat.1004905. PubMed PMID:  
951 26018192; PubMed Central PMCID: PMCPMC4446032.
- 952 21. Zheng W, Liu F, He Y, Liu Q, Humphreys GB, Tsuboi T, et al. Functional characterization  
953 of *Plasmodium berghei* PSOP25 during ookinete development and as a malaria transmission-  
954 blocking vaccine candidate. *Parasit Vectors.* 2017;10(1):8. Epub 2017/01/07. doi: 10.1186/s13071-  
955 016-1932-4. PubMed PMID: 28057055; PubMed Central PMCID: PMCPMC5217559.
- 956 22. Janse CJ, Franke-Fayard B, Mair GR, Ramesar J, Thiel C, Engelmann S, et al. High  
957 efficiency transfection of *Plasmodium berghei* facilitates novel selection procedures.  
958 *Molecular and biochemical parasitology.* 2006;145(1):60-70.
- 959 23. Annoura T, van Schaijk BC, Ploemen IH, Sajid M, Lin JW, Vos MW, et al. Two  
960 *Plasmodium* 6-Cys family-related proteins have distinct and critical roles in liver-stage  
961 development. *FASEB J.* 2014;28(5):2158-70. doi: 10.1096/fj.13-241570. PubMed PMID:  
962 24509910.
- 963 24. Feldmann AM, Ponnudurai T. Selection of *Anopheles stephensi* for refractoriness and  
964 susceptibility to *Plasmodium falciparum*. *Med Vet Entomol.* 1989;3(1):41-52. Epub 1989/01/01.  
965 PubMed PMID: 2519646.
- 966 25. Dong Y, Aguilar R, Xi Z, Warr E, Mongin E, Dimopoulos G. *Anopheles gambiae* immune  
967 responses to human and rodent *Plasmodium* parasite species. *PLoS Pathog.* 2006;2(6):e52. doi:  
968 10.1371/journal.ppat.0020052. PubMed PMID: 16789837; PubMed Central PMCID:  
969 PMCPMC1475661.
- 970 26. Dong Y, Dimopoulos G. *Anopheles* fibrinogen-related proteins provide expanded pattern  
971 recognition capacity against bacteria and malaria parasites. *J Biol Chem.* 2009;284(15):9835-44.  
972 doi: 10.1074/jbc.M807084200. PubMed PMID: 19193639; PubMed Central PMCID:  
973 PMCPMC2665105.
- 974 27. Srinivasan P, Fujioka H, Jacobs-Lorena M. PbCap380, a novel oocyst capsule protein, is  
975 essential for malaria parasite survival in the mosquito. *Cell Microbiol.* 2008;10(6):1304-12. Epub  
976 2008/02/06. doi: 10.1111/j.1462-5822.2008.01127.x. PubMed PMID: 18248630; PubMed Central  
977 PMCID: PMCPMC4137771.
- 978 28. Castillo JC, Ferreira ABB, Trisnadi N, Barillas-Mury C. Activation of mosquito  
979 complement antiplasmodial response requires cellular immunity. *Sci Immunol.* 2017;2(7). Epub  
980 2017/07/25. doi: 10.1126/sciimmunol.aal1505. PubMed PMID: 28736767; PubMed Central  
981 PMCID: PMCPMC5520810.

- 982 29. Frolet C, Thoma M, Blandin S, Hoffmann JA, Levashina EA. Boosting NF-kappaB-  
983 dependent basal immunity of *Anopheles gambiae* aborts development of *Plasmodium berghei*.  
984 Immunity. 2006;25(4):677-85. doi: 10.1016/j.immuni.2006.08.019. PubMed PMID: 17045818.
- 985 30. Smith RC, Barillas-Mury C, Jacobs-Lorena M. Hemocyte differentiation mediates the  
986 mosquito late-phase immune response against *Plasmodium* in *Anopheles gambiae*. Proc Natl Acad  
987 Sci U S A. 2015;112(26):E3412-20. doi: 10.1073/pnas.1420078112. PubMed PMID: 26080400;  
988 PubMed Central PMCID: PMC4491748.
- 989 31. Manske M, Miotto O, Campino S, Auburn S, Almagro-Garcia J, Maslen G, et al. Analysis  
990 of *Plasmodium falciparum* diversity in natural infections by deep sequencing. Nature.  
991 2012;487(7407):375-9. Epub 2012/06/23. doi: 10.1038/nature11174. PubMed PMID: 22722859;  
992 PubMed Central PMCID: PMC3738909.
- 993 32. Molina-Cruz A, Canepa GE, Barillas-Mury C. *Plasmodium P47*: a key gene for malaria  
994 transmission by mosquito vectors. Curr Opin Microbiol. 2017;40:168-74. Epub 2017/12/13. doi:  
995 10.1016/j.mib.2017.11.029. PubMed PMID: 29229188; PubMed Central PMCID:  
996 PMC5739336.
- 997 33. Molina-Cruz A, Canepa GE, Kamath N, Pavlovic NV, Mu J, Ramphul UN, et al.  
998 *Plasmodium* evasion of mosquito immunity and global malaria transmission: The lock-and-key  
999 theory. Proc Natl Acad Sci U S A. 2015;112(49):15178-83. doi: 10.1073/pnas.1520426112.  
1000 PubMed PMID: 26598665; PubMed Central PMCID: PMC4679011.
- 1001 34. Anthony TG, Polley SD, Vogler AP, Conway DJ. Evidence of non-neutral polymorphism in  
1002 *Plasmodium falciparum* gamete surface protein genes *Pfs47* and *Pfs48/45*. Mol Biochem Parasitol.  
1003 2007;156(2):117-23. doi: 10.1016/j.molbiopara.2007.07.008. PubMed PMID: 17826852.
- 1004 35. Eldering M, Morlais I, van Gemert GJ, van de Vegte-Bolmer M, Graumans W, Siebelink-  
1005 Stoter R, et al. Variation in susceptibility of African *Plasmodium falciparum* malaria parasites to  
1006 TEP1 mediated killing in *Anopheles gambiae* mosquitoes. Sci Rep. 2016;6:20440. doi:  
1007 10.1038/srep20440. PubMed PMID: 26861587; PubMed Central PMCID: PMC4748223.
- 1008 36. Canepa GE, Molina-Cruz A, Barillas-Mury C. Molecular Analysis of *Pfs47*-Mediated  
1009 *Plasmodium* Evasion of Mosquito Immunity. PLoS One. 2016;11(12):e0168279. Epub 2016/12/20.  
1010 doi: 10.1371/journal.pone.0168279. PubMed PMID: 27992481; PubMed Central PMCID:  
1011 PMC5167319.
- 1012 37. White BJ, Lawniczak MK, Cheng C, Coulibaly MB, Wilson MD, Sagnon N, et al. Adaptive  
1013 divergence between incipient species of *Anopheles gambiae* increases resistance to *Plasmodium*.  
1014 Proc Natl Acad Sci U S A. 2011;108(1):244-9. Epub 2010/12/22. doi: 10.1073/pnas.1013648108.  
1015 PubMed PMID: 21173248; PubMed Central PMCID: PMC3017163.
- 1016 38. Kaindoa EW, Matowo NS, Ngowo HS, Mkandawile G, Mmbando A, Finda M, et al.  
1017 Interventions that effectively target *Anopheles funestus* mosquitoes could significantly improve  
1018 control of persistent malaria transmission in south-eastern Tanzania. PLoS One.  
1019 2017;12(5):e0177807. Epub 2017/05/26. doi: 10.1371/journal.pone.0177807. PubMed PMID:  
1020 28542335; PubMed Central PMCID: PMC5436825.
- 1021 39. Habtewold T, Groom Z, Christophides GK. Immune resistance and tolerance strategies in  
1022 malaria vector and non-vector mosquitoes. Parasit Vectors. 2017;10(1):186. Epub 2017/04/20. doi:  
1023 10.1186/s13071-017-2109-5. PubMed PMID: 28420446; PubMed Central PMCID:  
1024 PMC5395841.
- 1025 40. Cuamba N, Mendis C. The role of *Anopheles merus* in malaria transmission in an area of  
1026 southern Mozambique. J Vector Borne Dis. 2009;46(2):157-9. Epub 2009/06/09. PubMed PMID:  
1027 19502697.

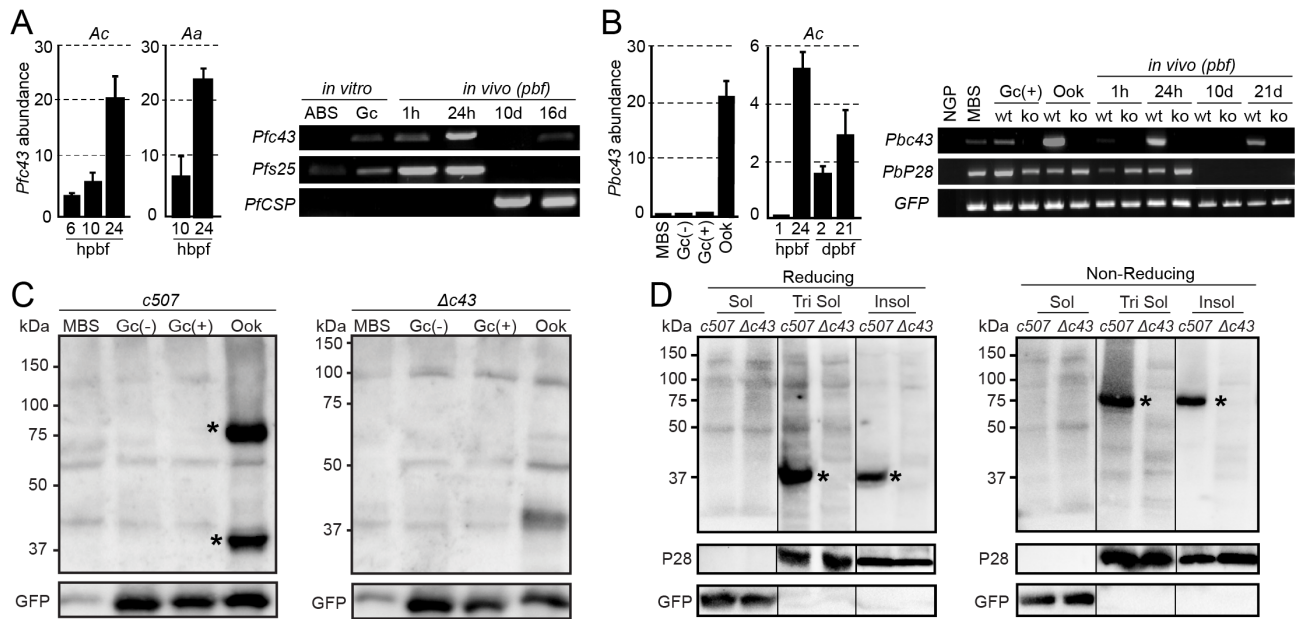
- 1028 41. Habtewold T, Tapanelli S, Masters EKG, Hoermann A, Windbichler N, Christophides GK.  
1029 Streamlined SMFA and mosquito dark-feeding regime significantly improve malaria transmission-  
1030 blocking assay robustness and sensitivity. *Malar J.* 2019;18(1):24. Epub 2019/01/27. doi:  
1031 10.1186/s12936-019-2663-8. PubMed PMID: 30683107; PubMed Central PMCID:  
1032 PMC6347765.
- 1033 42. Canepa GE, Molina-Cruz A, Yenkoidiok-Douti L, Calvo E, Williams AE, Burkhardt M, et  
1034 al. Antibody targeting of a specific region of Pfs47 blocks *Plasmodium falciparum* malaria  
1035 transmission. *NPJ Vaccines.* 2018;3:26. Epub 2018/07/14. doi: 10.1038/s41541-018-0065-5.  
1036 PubMed PMID: 30002917; PubMed Central PMCID: PMC639440.
- 1037 43. van Schaijk BC, van Dijk MR, van de Vegte-Bolmer M, van Gemert GJ, van Dooren MW,  
1038 Eksi S, et al. Pfs47, paralog of the male fertility factor Pfs48/45, is a female specific surface protein  
1039 in *Plasmodium falciparum*. *Mol Biochem Parasitol.* 2006;149(2):216-22. doi:  
1040 10.1016/j.molbiopara.2006.05.015. PubMed PMID: 16824624.
- 1041 44. Armistead JS, Morlais I, Mathias DK, Jardim JG, Joy J, Fridman A, et al. Antibodies to a  
1042 single, conserved epitope in *Anopheles APN1* inhibit universal transmission of *Plasmodium*  
1043 *falciparum* and *Plasmodium vivax* malaria. *Infect Immun.* 2014;82(2):818-29. Epub 2014/01/31.  
1044 doi: 10.1128/IAI.01222-13. PubMed PMID: 24478095; PubMed Central PMCID:  
1045 PMC63911399.
- 1046 45. Bustamante PJ, Woodruff DC, Oh J, Keister DB, Muratova O, Williamson KC. Differential  
1047 ability of specific regions of *Plasmodium falciparum* sexual-stage antigen, Pfs230, to induce  
1048 malaria transmission-blocking immunity. *Parasite Immunol.* 2000;22(8):373-80. Epub 2000/09/06.  
1049 PubMed PMID: 10972844.
- 1050 46. Zheng W, Kou X, Du Y, Liu F, Yu C, Tsuboi T, et al. Identification of three ookinete-  
1051 specific genes and evaluation of their transmission-blocking potentials in *Plasmodium berghei*.  
1052 *Vaccine.* 2016;34(23):2570-8. Epub 2016/04/17. doi: 10.1016/j.vaccine.2016.04.011. PubMed  
1053 PMID: 27083421; PubMed Central PMCID: PMC6347765.
- 1054 47. Naik RS, Branch OH, Woods AS, Vijaykumar M, Perkins DJ, Nahlen BL, et al.  
1055 Glycosylphosphatidylinositol anchors of *Plasmodium falciparum*: molecular characterization and  
1056 naturally elicited antibody response that may provide immunity to malaria pathogenesis. *J Exp*  
1057 *Med.* 2000;192(11):1563-76. Epub 2000/12/06. PubMed PMID: 11104799; PubMed Central  
1058 PMCID: PMC6347765.
- 1059 48. Arrighi RB, Faye I. *Plasmodium falciparum* GPI toxin: a common foe for man and  
1060 mosquito. *Acta Trop.* 2010;114(3):162-5. Epub 2009/06/23. doi: 10.1016/j.actatropica.2009.06.003.  
1061 PubMed PMID: 19539593.
- 1062 49. Lim J, Gowda DC, Krishnegowda G, Luckhart S. Induction of nitric oxide synthase in  
1063 *Anopheles stephensi* by *Plasmodium falciparum*: mechanism of signaling and the role of parasite  
1064 glycosylphosphatidylinositols. *Infect Immun.* 2005;73(5):2778-89. Epub 2005/04/23. doi:  
1065 10.1128/IAI.73.5.2778-2789.2005. PubMed PMID: 15845481; PubMed Central PMCID:  
1066 PMC6347765.
- 1067 50. Poole LB. The basics of thiols and cysteines in redox biology and chemistry. *Free Radic*  
1068 *Biol Med.* 2015;80:148-57. Epub 2014/11/30. doi: 10.1016/j.freeradbiomed.2014.11.013. PubMed  
1069 PMID: 25433365; PubMed Central PMCID: PMC6347765.
- 1070 51. Molina-Cruz A, DeJong RJ, Charles B, Gupta L, Kumar S, Jaramillo-Gutierrez G, et al.  
1071 Reactive oxygen species modulate *Anopheles gambiae* immunity against bacteria and *Plasmodium*.  
1072 *J Biol Chem.* 2008;283(6):3217-23. doi: 10.1074/jbc.M705873200. PubMed PMID: 18065421.



- 1073 52. Sinden RE. Infection of mosquitoes with rodent malaria. The molecular biology of insect  
1074 disease vectors: Springer; 1997. p. 67-91.
- 1075 53. Chaturvedi N, Bharti PK, Tiwari A, Singh N. Strategies & recent development of  
1076 transmission-blocking vaccines against *Plasmodium falciparum*. Indian J Med Res.  
1077 2016;143(6):696-711. Epub 2016/10/18. doi: 10.4103/0971-5916.191927. PubMed PMID:  
1078 27748294; PubMed Central PMCID: PMC5094109.
- 1079 54. Gantz VM, Jasinskiene N, Tatarenkova O, Fazekas A, Macias VM, Bier E, et al. Highly  
1080 efficient Cas9-mediated gene drive for population modification of the malaria vector mosquito  
1081 *Anopheles stephensi*. Proc Natl Acad Sci U S A. 2015;112(49):E6736-43. Epub 2015/11/26. doi:  
1082 10.1073/pnas.1521077112. PubMed PMID: 26598698; PubMed Central PMCID:  
1083 PMC4679060.
- 1084 55. Isaacs AT, Li F, Jasinskiene N, Chen X, Nirmala X, Marinotti O, et al. Engineered  
1085 resistance to *Plasmodium falciparum* development in transgenic *Anopheles stephensi*. PLoS Pathog.  
1086 2011;7(4):e1002017. Epub 2011/05/03. doi: 10.1371/journal.ppat.1002017. PubMed PMID:  
1087 21533066; PubMed Central PMCID: PMC3080844.
- 1088 56. Carballar-Lejarazu R, James AA. Population modification of Anopheline species to control  
1089 malaria transmission. Pathog Glob Health. 2017;111(8):424-35. Epub 2018/02/02. doi:  
1090 10.1080/20477724.2018.1427192. PubMed PMID: 29385893; PubMed Central PMCID:  
1091 PMC6066855.
- 1092 57. Petersen TN, Brunak S, von Heijne G, Nielsen H. SignalP 4.0: discriminating signal  
1093 peptides from transmembrane regions. Nat Methods. 2011;8(10):785-6. Epub 2011/10/01. doi:  
1094 10.1038/nmeth.1701. PubMed PMID: 21959131.
- 1095 58. Moller S, Croning MD, Apweiler R. Evaluation of methods for the prediction of membrane  
1096 spanning regions. Bioinformatics. 2001;17(7):646-53. Epub 2001/07/13. PubMed PMID:  
1097 11448883.
- 1098 59. Dearsly AL, Sinden RE, Self IA. Sexual development in malarial parasites: gametocyte  
1099 production, fertility and infectivity to the mosquito vector. Parasitology. 1990;100 Pt 3:359-68.  
1100 Epub 1990/06/01. PubMed PMID: 2194152.
- 1101 60. Winger LA, Tirawanchai N, Nicholas J, Carter HE, Smith JE, Sinden RE. Ookinete antigens  
1102 of *Plasmodium berghei*. Appearance on the zygote surface of an Mr 21 kD determinant identified  
1103 by transmission-blocking monoclonal antibodies. Parasite Immunol. 1988;10(2):193-207. Epub  
1104 1988/03/01. PubMed PMID: 2453831.
- 1105 61. Barr PJ, Green KM, Gibson HL, Bathurst IC, Quakyi IA, Kaslow DC. Recombinant Pfs25  
1106 protein of *Plasmodium falciparum* elicits malaria transmission-blocking immunity in experimental  
1107 animals. J Exp Med. 1991;174(5):1203-8. Epub 1991/11/01. PubMed PMID: 1940798; PubMed  
1108 Central PMCID: PMC2118997.
- 1109 62. Zavala F, Cochrane AH, Nardin EH, Nussenzweig RS, Nussenzweig V. Circumsporozoite  
1110 proteins of malaria parasites contain a single immunodominant region with two or more identical  
1111 epitopes. J Exp Med. 1983;157(6):1947-57. Epub 1983/06/01. PubMed PMID: 6189951; PubMed  
1112 Central PMCID: PMC2187031.
- 1113 63. Potocnjak P, Yoshida N, Nussenzweig RS, Nussenzweig V. Monovalent fragments (Fab) of  
1114 monoclonal antibodies to a sporozoite surface antigen (Pb44) protect mice against malarial  
1115 infection. J Exp Med. 1980;151(6):1504-13. Epub 1980/06/01. PubMed PMID: 6991628; PubMed  
1116 Central PMCID: PMC2185881.
- 1117 64. Dessens JT, Beetsma AL, Dimopoulos G, Wengelnik K, Crisanti A, Kafatos FC, et al.  
1118 CTRP is essential for mosquito infection by malaria ookinetes. EMBO J. 1999;18(22):6221-7. Epub

- 1119 1999/11/24. doi: 10.1093/emboj/18.22.6221. PubMed PMID: 10562534; PubMed Central PMCID:  
1120 PMCPMC1171685.
- 1121 65. Braks JA, Franke-Fayard B, Kroeze H, Janse CJ, Waters AP. Development and application  
1122 of a positive-negative selectable marker system for use in reverse genetics in *Plasmodium*. *Nucleic*  
1123 *Acids Res.* 2006;34(5):e39. Epub 2006/03/16. doi: 10.1093/nar/gnj033. PubMed PMID: 16537837;  
1124 PubMed Central PMCID: PMCPMC1401515.
- 1125 66. Moon RW, Taylor CJ, Bex C, Schepers R, Goulding D, Janse CJ, et al. A cyclic GMP  
1126 signalling module that regulates gliding motility in a malaria parasite. *PLoS Pathog.*  
1127 2009;5(9):e1000599. Epub 2009/09/26. doi: 10.1371/journal.ppat.1000599. PubMed PMID:  
1128 19779564; PubMed Central PMCID: PMCPMC2742896.
- 1129 67. Habtewold T, Povelones M, Blagborough AM, Christophides GK. Transmission blocking  
1130 immunity in the malaria non-vector mosquito *Anopheles quadriannulatus* species A. *PLoS Pathog.*  
1131 2008;4(5):e1000070. doi: 10.1371/journal.ppat.1000070. PubMed PMID: 18497855; PubMed  
1132 Central PMCID: PMCPMC2374904.
- 1133 68. Osta MA, Christophides GK, Kafatos FC. Effects of mosquito genes on *Plasmodium*  
1134 development. *Science.* 2004;303(5666):2030-2. doi: 10.1126/science.1091789. PubMed PMID:  
1135 15044804.
- 1136 69. Bushell ES, Ecker A, Schlegelmilch T, Goulding D, Dougan G, Sinden RE, et al. Paternal  
1137 effect of the nuclear formin-like protein MISFIT on *Plasmodium* development in the mosquito  
1138 vector. *PLoS pathogens.* 2009;5(8):e1000539. Epub 2009/08/08. doi:  
1139 10.1371/journal.ppat.1000539. PubMed PMID: 19662167; PubMed Central PMCID:  
1140 PMC2715856.
- 1141 70. Kim D, Langmead B, Salzberg SL. HISAT: a fast spliced aligner with low memory  
1142 requirements. *Nat Methods.* 2015;12(4):357-60. Epub 2015/03/10. doi: 10.1038/nmeth.3317.  
1143 PubMed PMID: 25751142; PubMed Central PMCID: PMCPMC4655817.
- 1144 71. Giraldo-Calderon GI, Emrich SJ, MacCallum RM, Maslen G, Dialynas E, Topalis P, et al.  
1145 VectorBase: an updated bioinformatics resource for invertebrate vectors and other organisms  
1146 related with human diseases. *Nucleic Acids Res.* 2015;43(Database issue):D707-13. Epub  
1147 2014/12/17. doi: 10.1093/nar/gku1117. PubMed PMID: 25510499; PubMed Central PMCID:  
1148 PMCPMC4383932.
- 1149 72. Bahl A, Brunk B, Crabtree J, Fraunholz MJ, Gajria B, Grant GR, et al. PlasmoDB: the  
1150 *Plasmodium* genome resource. A database integrating experimental and computational data.  
1151 *Nucleic Acids Res.* 2003;31(1):212-5. Epub 2003/01/10. PubMed PMID: 12519984; PubMed  
1152 Central PMCID: PMCPMC165528.
- 1153 73. Trapnell C, Williams BA, Pertea G, Mortazavi A, Kwan G, van Baren MJ, et al. Transcript  
1154 assembly and quantification by RNA-Seq reveals unannotated transcripts and isoform switching  
1155 during cell differentiation. *Nat Biotechnol.* 2010;28(5):511-5. Epub 2010/05/04. doi:  
1156 10.1038/nbt.1621. PubMed PMID: 20436464; PubMed Central PMCID: PMCPMC3146043.
- 1157 74. Trapnell C, Hendrickson DG, Sauvageau M, Goff L, Rinn JL, Pachter L. Differential  
1158 analysis of gene regulation at transcript resolution with RNA-seq. *Nat Biotechnol.* 2013;31(1):46-  
1159 53. Epub 2012/12/12. doi: 10.1038/nbt.2450. PubMed PMID: 23222703; PubMed Central PMCID:  
1160 PMCPMC3869392.
- 1161 75. Afgan E, Baker D, van den Beek M, Blankenberg D, Bouvier D, Cech M, et al. The Galaxy  
1162 platform for accessible, reproducible and collaborative biomedical analyses: 2016 update. *Nucleic*  
1163 *Acids Res.* 2016;44(W1):W3-W10. Epub 2016/05/04. doi: 10.1093/nar/gkw343. PubMed PMID:  
1164 27137889; PubMed Central PMCID: PMCPMC4987906.

- 1165 76. Hart T, Komori HK, LaMere S, Podshivalova K, Salomon DR. Finding the active genes in  
1166 deep RNA-seq gene expression studies. *BMC Genomics*. 2013;14:778. Epub 2013/11/13. doi:  
1167 10.1186/1471-2164-14-778. PubMed PMID: 24215113; PubMed Central PMCID:  
1168 PMCPMC3870982.
- 1169 77. Mi H, Muruganujan A, Thomas PD. PANTHER in 2013: modeling the evolution of gene  
1170 function, and other gene attributes, in the context of phylogenetic trees. *Nucleic Acids Res*.  
1171 2013;41(Database issue):D377-86. Epub 2012/11/30. doi: 10.1093/nar/gks1118. PubMed PMID:  
1172 23193289; PubMed Central PMCID: PMCPMC3531194.
- 1173 78. Zheng X, Levine D, Shen J, Gogarten SM, Laurie C, Weir BS. A high-performance  
1174 computing toolset for relatedness and principal component analysis of SNP data. *Bioinformatics*.  
1175 2012;28(24):3326-8. Epub 2012/10/13. doi: 10.1093/bioinformatics/bts606. PubMed PMID:  
1176 23060615; PubMed Central PMCID: PMCPMC3519454.
- 1177 79. Angrisano F, Sala KA, Da DF, Liu Y, Pei J, Grishin NV, et al. Targeting the Conserved  
1178 Fusion Loop of HAP2 Inhibits the Transmission of *Plasmodium berghei* and *falciparum*. *Cell Rep*.  
1179 2017;21(10):2868-78. Epub 2017/12/07. doi: 10.1016/j.celrep.2017.11.024. PubMed PMID:  
1180 29212032; PubMed Central PMCID: PMCPMC5732318.

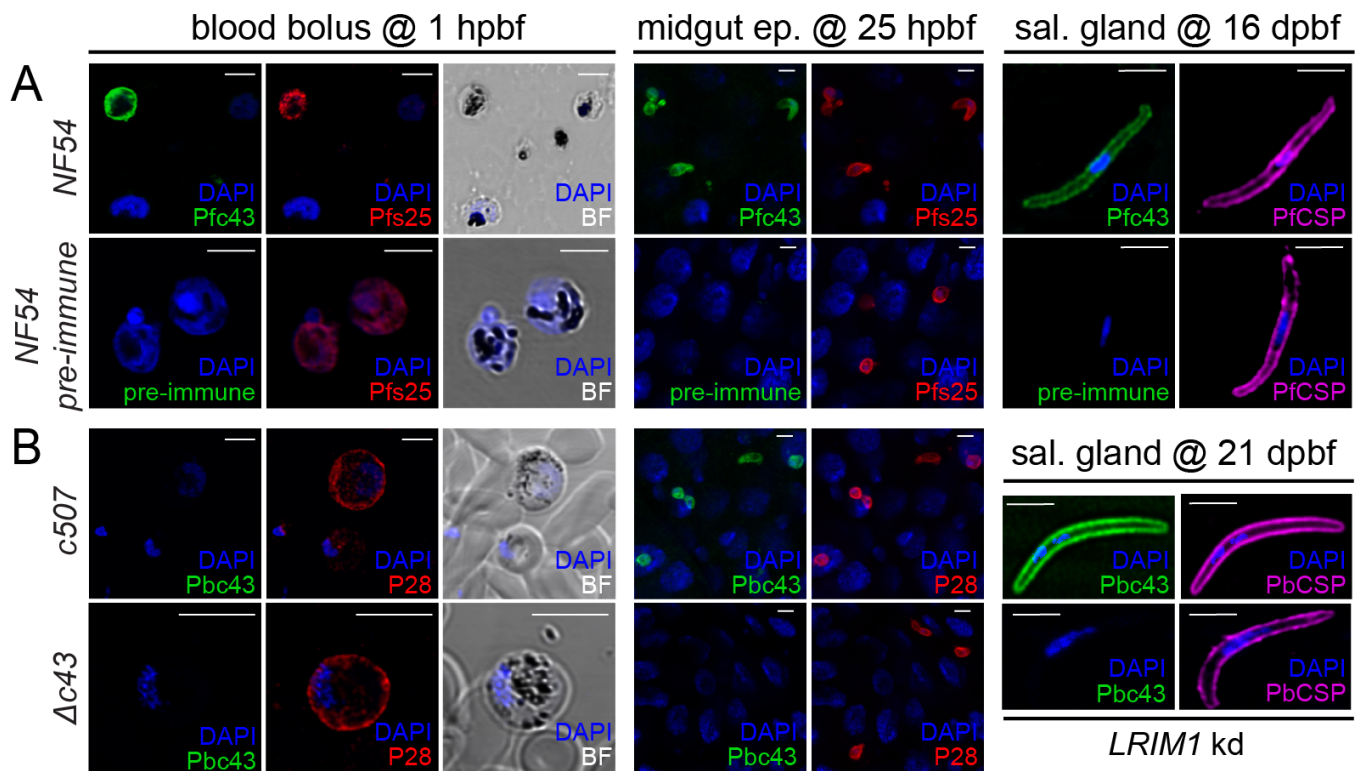


1181

1182 **Figure 1. PIMMS43 transcription profiles and protein expression**

1183 (A) Left panel: DNA microarray transcriptional profiling of *Pfc43* in *A. coluzzii* (*Ac*) and *A.*  
 1184 *arabiensis* (*Aa*) midguts. Bars show transcript abundance at indicated time points relative to 1 hpbf  
 1185 and are average of three biological replicates. Error bars show SEM. Right panel: RT-PCR analysis  
 1186 of *Pfc43* transcripts in *in vitro* and *in vivo* NF54 parasite populations. Gametocyte expressed gene  
 1187 *Pfs25* and sporozoite-expressed gene *PfCSP* serve as both stage-specific and loading controls. (B)  
 1188 Left panel: Relative abundance of *Pbc43* transcripts in blood stages, *in vitro* ookinetes, and *A.*  
 1189 *coluzzii* mosquito stages, as determined by qRT-PCR in the *c507* line and normalized against the  
 1190 constitutive expressed *GFP*. Each bar is the average of three biological replicates. Error bars show  
 1191 SEM. Right panel: RT-PCR analysis of the expression of *Pbc43* transcripts in blood stages, *in vitro*  
 1192 ookinetes and *A. coluzzii* mosquito stages. Gametocyte expressed gene *P28* and constitutive  
 1193 expressed *GFP* served as a stage-specific and loading controls, respectively.  $\Delta c43$  parasites were  
 1194 used as a negative control. (C) Western blot analysis under reducing conditions using the  $\alpha$ -Pbc43<sup>opt</sup>  
 1195 antibody on whole cell lysates of *c507* parasites. Pbc43 protein bands are indicated with asterisks.  
 1196  $\Delta c43$  parasites were used as a negative control. GFP was used as a loading control. (D) Western  
 1197 blot analysis under reducing (left panel) and non-reducing (right panel) conditions using the  $\alpha$ -  
 1198 Pbc43<sup>opt</sup> antibody on fractionated *in vitro* ookinetes. Pbc43 protein bands are indicated with  
 1199 asterisks.  $\Delta c43$  ookinetes were used as a negative control. *P28* and *GFP* were used as stage-specific  
 1200 and loading controls, respectively. Soluble (Sol), Triton soluble (Tri Sol) and insoluble (Insol)  
 1201 fractions are shown. Abbreviations: ABS, asexual blood stages; NGP, non-gametocyte producing;  
 1202 MBS, mixed blood stages; Gc, gametocytes; Gc (-), non-activated gametocytes; Gc (+), activated  
 1203 gametocytes; Ook, ookinetes; pbf, post blood feeding.

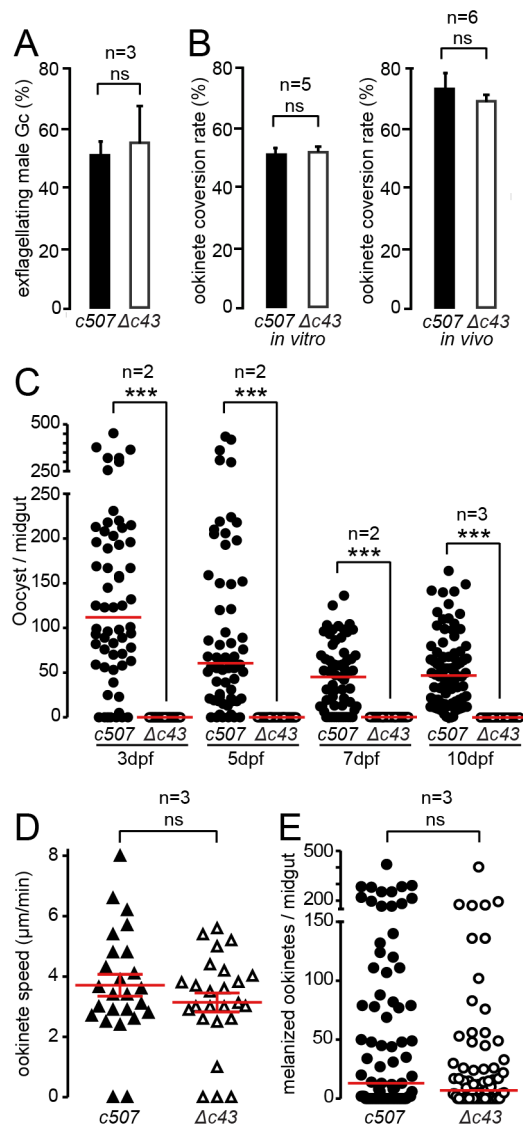




1204

1205 **Figure 2. PIMMS43 protein localization**

1206 (A) Immunofluorescence assays of *P. falciparum* NF54 parasites found in mosquito blood bolus of  
 1207 at 1 hpb (left), ookinets traversing the mosquito midgut epithelium at 25 hpb (middle), and  
 1208 salivary gland sporozoites at 16 dpb (right panel), stained with  $\alpha$ -Pfc43<sup>opt</sup> (green) and the female  
 1209 gamete/zygote/ookinete  $\alpha$ -Pfs25 (red) or sporozoite  $\alpha$ -PfcCSP (purple) antibodies. DNA was stained  
 1210 with DAPI. Staining with pre-immune serum was used as a negative control. (B)  
 1211 Immunofluorescence assays of *P. berghei* 507 early sexual stages (activated gametocytes and/or  
 1212 early zygotes) in mosquito blood bolus at 1 hpb (left), ookinets traversing the mosquito midgut  
 1213 epithelium at 25 hpb (middle) and salivary gland sporozoites at 21 dpb (right), stained with  
 1214  $\alpha$ -Pbc43<sup>opt</sup> (green), female gamete/zygote/ookinete surface  $\alpha$ -P28 (red) or sporozoite surface  
 1215  $\alpha$ -PbCSP (purple) antibodies. DNA was stained with DAPI. Staining of the  $\Delta c43$  parasite with  
 1216  $\alpha$ -Pbc43<sup>opt</sup> was used as a negative control. Note that  $\Delta c43$  sporozoites were obtained from  
 1217 infections of *LRIM1* kd mosquitoes. Images are de-convoluted projection of confocal stacks. BF  
 1218 denotes bright field and scale bars correspond to 5  $\mu$ m.

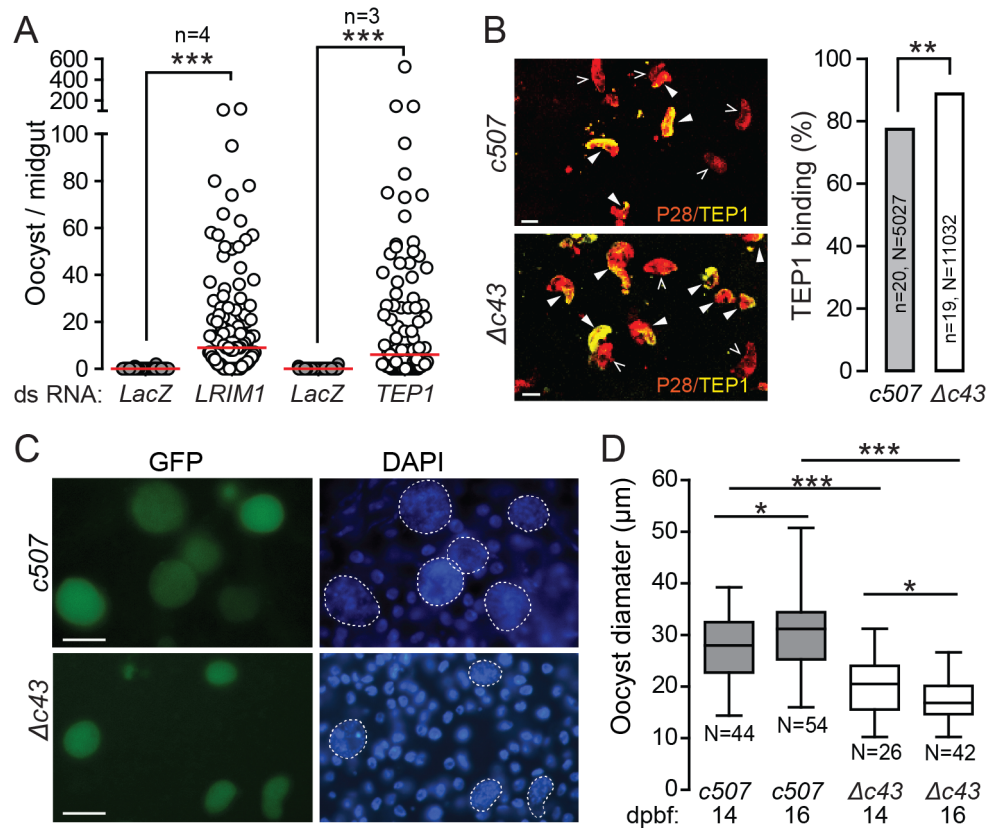


1219

1220 **Figure 3. Phenotypic analysis of *P. berghei*  $\Delta c43$  knock out mutant parasites**

1221 Male gametocyte activation measured as percentage of exflagellating male gametocytes (A) and  
 1222 female gamete conversion to ookinetes *in vitro* (left), and *in vivo* in the *A. coluzzii* midgut of (right)  
 1223 (B) of *c507 wt* and  $\Delta c43$  parasites. Error bars show SEM. (C)  $\Delta c43$  oocyst development at 3, 5, 7  
 1224 and 10 dpbf in *A. coluzzii*. \*\*\*,  $P < 0.0001$ , Mann-Whitney test. (D) Speed of *c507 wt* and  $\Delta c43$   
 1225 ookinetes measured from time-lapse microscopy, captured at 1 frame/5 sec for 10 min. Red lines  
 1226 indicate mean and error bars show SEM. (E) Melanized ookinete numbers in *CTL4 kd A. coluzzii*  
 1227 infected with *c507 wt* and  $\Delta c43$  parasite lines. Red lines indicate median; ns, not significant; n,  
 1228 number of biological replicates.

1229

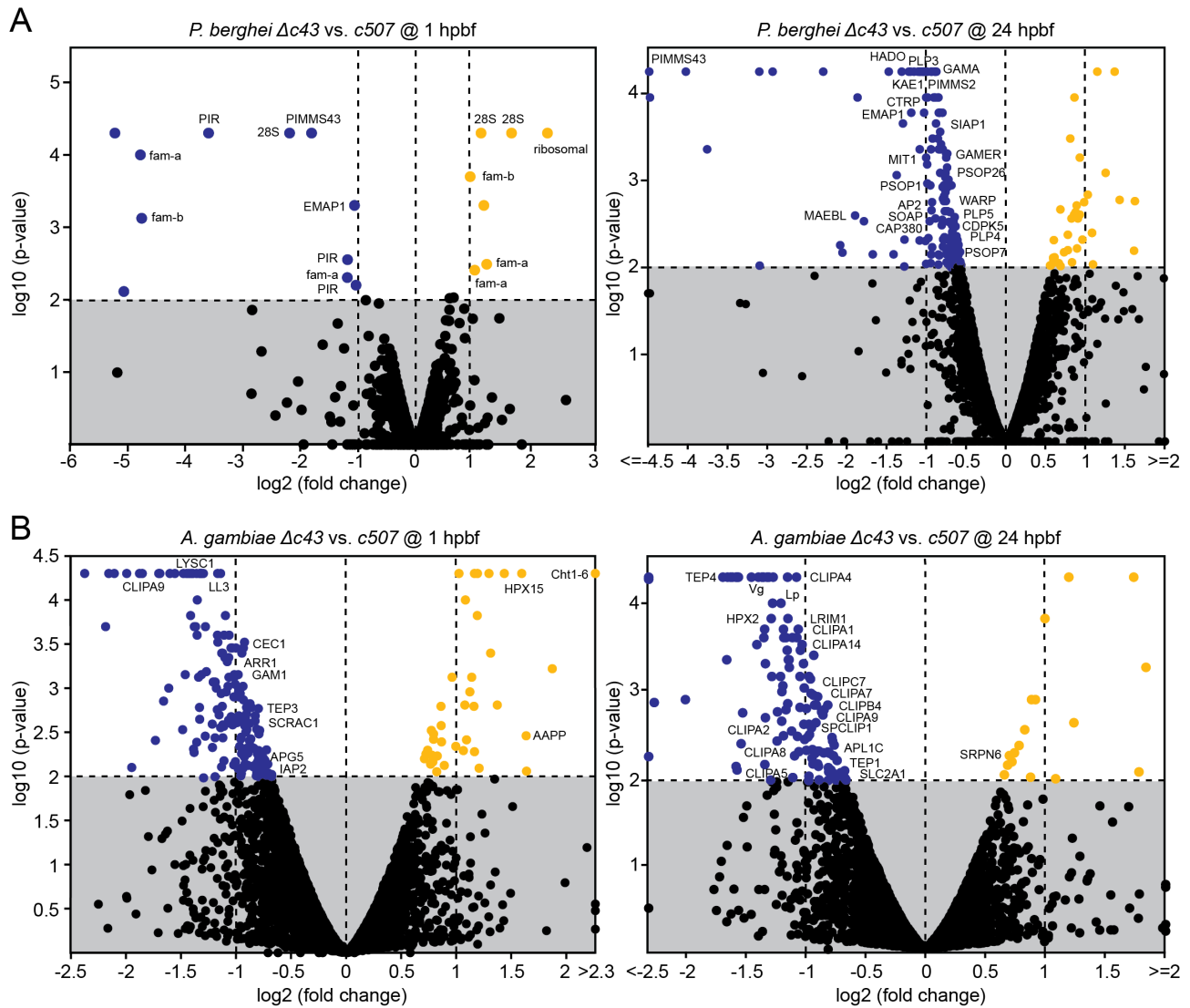


1230

1231 **Figure 4. Effect of *A. coluzzii* immune response on *P. berghei*  $\Delta c43$  mutants**

1232 **(A)** Effect of *LRIM1* and *TEP1* silencing on  $\Delta c43$  oocyst numbers in *A. coluzzii* midguts. *dsLacZ*  
1233 injected mosquitoes were used as controls. Red lines indicates median; n, number of independent  
1234 experiments; \*\*\*,  $P < 0.0001$ , Mann-Whitney test. **(B)** *c507* wt and  $\Delta c43$  ookinete killing by  
1235 complement-like reactions in *A. coluzzii* midgut. Representative images of tissues stained with P28  
1236 (red) and TEP1 (yellow) antibodies (left). P28 staining marks all ookinetes (both open and filled  
1237 arrowheads) and double TEP1/P28 staining marks ookinetes that are either killed or in the process  
1238 of being killed (filled arrowheads). Images are projection of confocal stacks taken at 400X  
1239 magnification. Scale bar is 5 μm. The percentage of TEP1/P28 double-stained ookinetes is shown in  
1240 the graph on the right, where n is number of midguts analyzed in 3 independent biological  
1241 experiments and N is number of ookinetes. \*\*,  $P < 0.001$ , unpaired Student's *t*-test. **(C)**  
1242 Representative images of rescued  $\Delta c43$  oocysts in *LRIM1* kd mosquitoes showing variable  
1243 morphology and smaller size compared to *c507* wt oocysts. Scale bar is 30 μm. **(D)** Box plot of  
1244 diameter measurements of  $\Delta c43$  and *c507* wt oocysts at 14 and 16 dpbf. Upper and lower whiskers  
1245 represent the largest and smallest oocyst diameter, respectively. Horizontal line in each box  
1246 indicates mean of 2 biological replicates and whiskers show SEM. N is number of oocysts; \*,  
1247  $P < 0.05$ , and \*\*\*,  $P < 0.0001$  using unpaired Student's *t*-test.

1248



1249

1250

**Figure 5. *P. berghei* and *A. coluzzii* gene expression**

1251

1252

1253

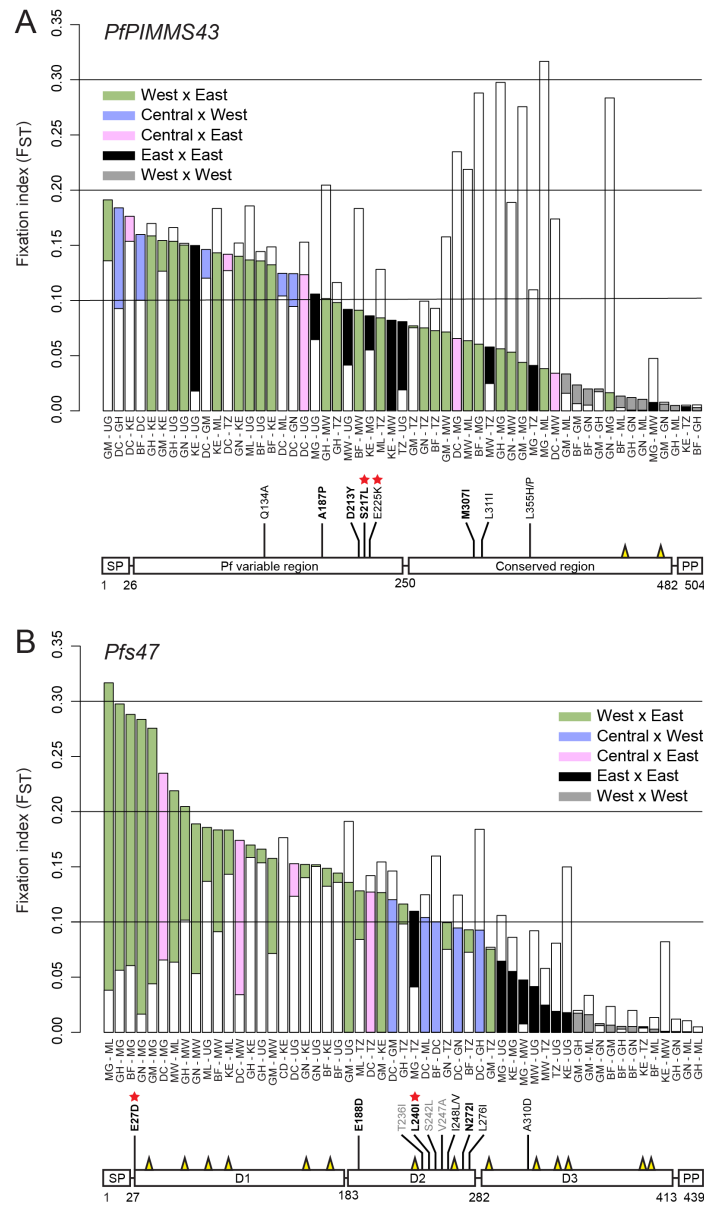
1254

1255

1256

(A) Volcano plots of *P. berghei* gene expression in  $\Delta c43$  vs. *c507* *wt* parasite lines in the *A. coluzzii* midgut at 1 (left) and 24 (right) hpbpf. (B) Volcano plots of *A. coluzzii* midgut transcriptional responses to  $\Delta c43$  vs. *c507* *wt* parasites at 1 (left) and 24 (right) hpbpf. X-axes show  $\log_2$  fold change and y-axes show  $\log_{10}$  p-value calculated using one-way ANOVA. Blue and orange filled circles indicate genes that are at least 2-fold downregulated and 2-fold upregulated, respectively. Black circles show with no significant differential regulation. Known gene names are indicated.

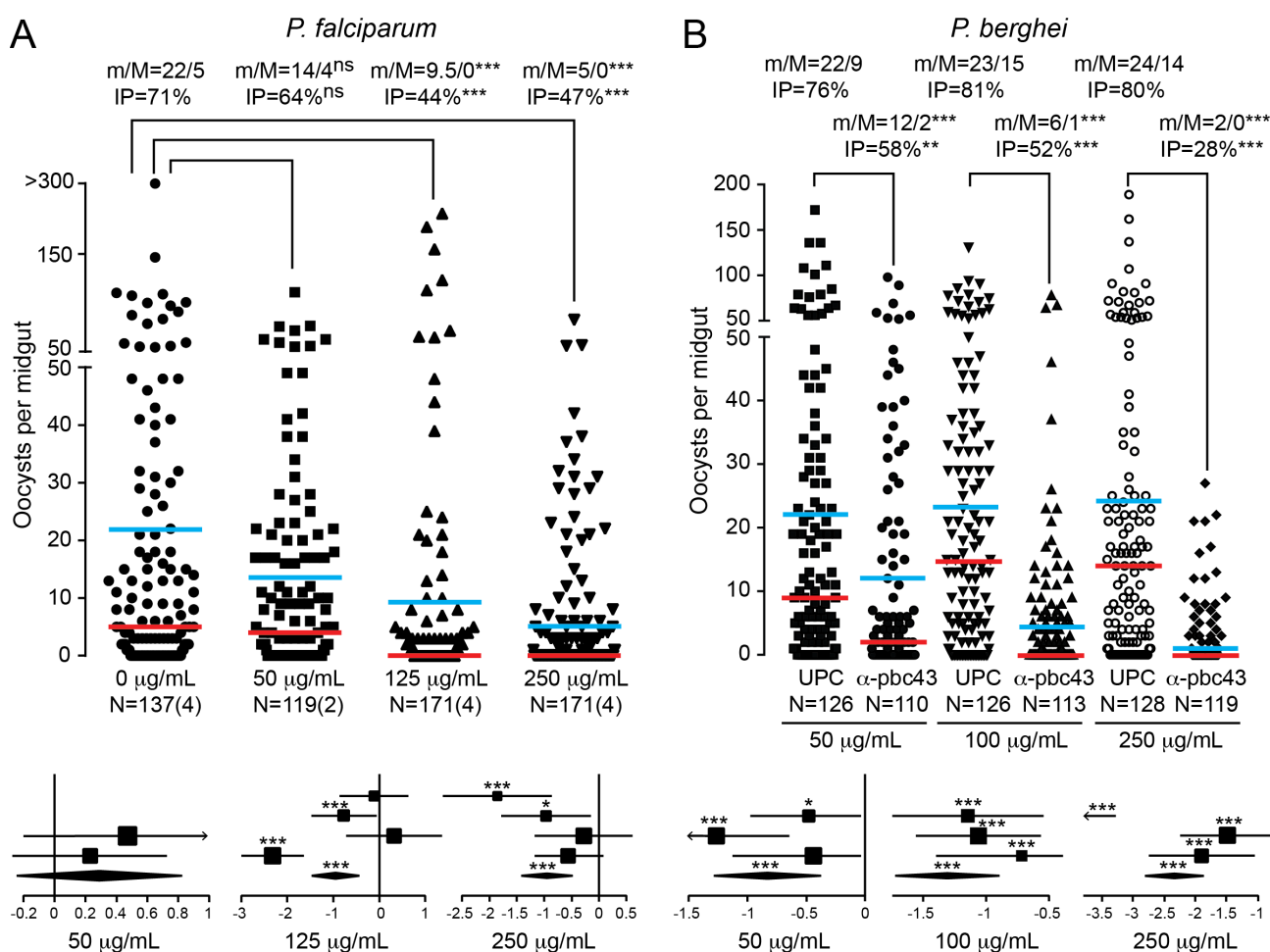




1257

1258 **Figure 6. Population genetic analysis of PIMMS43 and P47 in African *P. falciparum***

1259 *PfPIMMS43* (A) and *Pfs47* (B) fixation index ( $F_{ST}$ ) values of 1,509 *P. falciparum* populations  
 1260 sampled from patients across Africa (top panels) and schematic representation of SNPs with high  
 1261  $F_{ST}$  values leading to amino acid substitutions in each deduced protein (bottom panels). In top  
 1262 panels, colour coding indicates comparisons between countries in West, Central and East Africa.  
 1263 Central Africa includes populations sampled only from the Democratic Republic of the Congo.  
 1264 White bars overlaid with coloured bars in each of the gene graphs indicate the  $F_{ST}$  of the other gene,  
 1265 i.e. *Pfs47* in *PfPIMMS43* graph and *PfPIMMS43* in *Pfs47* graph. In bottom panels, boldfaced amino  
 1266 acid substitutions are those deriving from SNPs with total  $F_{ST}>0.1$ , and the rest of the substitutions  
 1267 are those showing high  $F_{ST}$  in comparisons between populations sampled from specific countries.  
 1268 Substitutions in *Pfs47* presented in grey do not show high  $F_{ST}$  but have been shown previously to be  
 1269 present in laboratory NF54 *P. falciparum* and be involved in parasite immune evasion. Substitutions  
 1270 marked with red stars are those showing very high  $F_{ST}$  and have swept to almost fixation in some  
 1271 populations. Yellow spikes show the positions of conserved Cysteine residues. Burkina Faso, BF;  
 1272 Democratic Republic of the Congo, DC; Gambia, GM; Ghana, GH; Guinea, GN; Kenya, KE;  
 1273 Madagascar, MG; Malawi, MW; Mali, ML; Tanzania, TZ; Uganda, UG.



1274

1275

### Figure 7. *P. falciparum* and *P. berghei* transmission blocking with anti-PIMMS43 antibodies

1276

1277 Transmission blocking efficacies of anti-PIMMS43 antibodies on *P. falciparum* (A) and *P. berghei*  
 1278 (**B**) infections of *A. coluzzii* shown as dot plots of oocyst number distribution (top panels) and  
 1279 forest plots of GLMM analysis (bottom panels). The  $\alpha$ -Pfc43<sup>opt</sup> and  $\alpha$ -Pbc43<sup>Sf9</sup> antibodies were provided  
 1280 through SMFAs at concentrations of 50, 125 and 250 µg/mL, and 50, 100 and 250 µg/mL,  
 1281 respectively, and compared with no antibodies and UPC10 antibodies that were used as negative  
 1282 controls for *P. falciparum* and *P. berghei*, respectively. Individual data points represent oocyst  
 1283 numbers from individual mosquitoes at 7 and 10 dpbf from 2/4 and 3 biological SMFA replicates  
 1284 with *P. falciparum* and *P. berghei*, respectively. m/M are mean/median oocyst infection intensities,  
 1285 also shown as horizontal blue and red lines, respectively. IP, oocyst infection prevalence; N,  
 1286 number of midguts analyzed; n, number of independent experiments; ns, not significant. Statistical  
 1287 analysis was performed with Mann-Whitney test for infection intensity and Fisher's exact test for  
 1288 infection prevalence; \*\*, P<0.005; \*\*\*, P<0.0001. In GLMM analyses, the variation of fixed effect  
 1289 estimates for each replicate (squares) and all replicates (diamonds) are shown ( $\pm$ 95% confidence  
 1290 interval, glmmADMB). The square size is proportional to the sum of midguts analysed in each  
 replicate. \*, P<0.05; \*\*\*, P<0.0001.